

An evidence clustering DSMT approximate reasoning method for more than two sources



Qiang Guo*, You He, Tao Jian*, Haipeng Wang, Shutao Xia

Research Institute of Information Fusion, Naval Aeronautical and Astronautical University, Yantai, Shandong 264001, China

ARTICLE INFO

Article history:

Available online 27 May 2016

Keywords:

Information fusion

Evidence theory

Approximate reasoning

Dezert–Smarandache Theory (DSMT)

Proportional Conflict Redistribution 6 (PCR6)

ABSTRACT

Due to the huge computation complexity of Dezert–Smarandache Theory (DSMT), its applications especially for multi-source (more than two sources) complex fusion problems have been limited. To get high similar approximate reasoning results with Proportional Conflict Redistribution 6 (PCR6) rule in DSMT framework (DSMT + PCR6) and remain less computation complexity, an Evidence Clustering DSMT approximate reasoning method for more than two sources is proposed. Firstly, the focal elements of multi evidences are clustered to two sets by their mass assignments respectively. Secondly, the convex approximate fusion results are obtained by the new DSMT approximate formula for more than two sources. Thirdly, the final approximate fusion results by the method in this paper are obtained by the normalization step. Analysis of computation complexity show that the method in this paper cost much less computation complexity than DSMT + PCR6. The simulation experiments show that the method in this paper can get very similar approximate fusion results and need much less computing time than DSMT + PCR6, especially, when the numbers of sources and focal elements are large, the superiorities of the method are remarkable.

© 2016 Elsevier Inc. All rights reserved.

1. Introduction

With the rapid development of science and technology, sensor types become diverse. To solve the more and more complex practical problems, information fusion from different multi sources has been drawn great attention by scholars in recent years [1–12]. Due to the influence of noise, uncertain signal and information processing has become an important research direction in the field of information fusion. Belief function theory (also called evidence theory) has played a key role in uncertain and even conflict information processing. As a traditional evidence theory, Dempster–Shafer theory (DST) [13,14] is a general applied information fusion method. However, DSMT, jointly proposed by Dezert and Smarandache [12], beyonds the exclusiveness limitation of DST and especially in highly conflict information cases, it can obtain more accurate fusion results than DST. Recently, DSMT has many successful applications, such as, Map Reconstruction of Robot [15], Decision Making Support [16,17], Target Type Tracking [18], Image Processing [19], Sonar Imagery [20], Data Classification [21–25], Clustering [26–28], and so on. Besides, neutrosopic theory [29–31] proposed by Smarandache is a novel effective uncertain information process-

ing method. However, the main problem of DSMT is that when the number of sources and focal elements increases, the computation complexity of PCR5 or PCR6 in DSMT framework increases exponentially [32].

There were some important methods for reducing the computation complexity of the combination algorithms in DSMT framework since this problem can be treated in different ways: 1) reducing the number of focal elements [33–36], 2) reducing the number of combined sources [37], 3) reducing both the number of focal elements and the number of combined sources [38]. Applied mathematics has drawn attention by many scholars [39,40]. Particularly, the very recent Evidence Clustering DSMT Approximate Reasoning Method based on Convex Function Analysis [11] proposed by Guo, He, et al can get very similar approximate fusion results with PCR5 in DSMT framework and cost little computation complexity. Nevertheless, the approximate method in [11] is only for two sources and it is not associative in the fusion of multiple (more than 2) sources of evidences.

For reducing the huge computation complexity of Dezert–Smarandache Theory (DSMT) for multi-source (more than two sources) complex fusion problems and get more similar approximate fusion results with PCR6 in DSMT framework (DSMT + PCR6), a DSMT Approximate Reasoning Method for More than Two Sources is proposed in this paper. In Section 2, the basics knowledge on DST, DSMT + PCR6 and evidential distance theory are in-

* Corresponding authors.

E-mail addresses: gq19860209@163.com (Q. Guo), jiantao_ythy@163.com (T. Jian).

troduced briefly. In Section 3, a new form of PCR6 formula is given and the mathematical analysis of the new form is conducted. Then a new DSMT approximate reasoning method for more than two sources is proposed. Finally, Analysis of computation complexity shows that the method in this paper costs much less computation complexity than DSMT + PCR6. In Section 4, the simulation experiments show that the method in this paper can get very similar approximate fusion results and need much less computing time than DSMT + PCR6, especially, when the number of sources and focal elements is large, the superiorities of the method are remarkable. In Section 5, the conclusions are given.

2. Basic knowledge

2.1. Dempster–Shafer theory (DST)

A discernment frame based on the Shafer's model is defined as $\Theta = \{\theta_1, \theta_2, \dots, \theta_n\}$ which contains n exclusive elements. The mass assignments of evidences defined over the power-set 2^Θ is defined by

$$m(X_i) : 2^\Theta \rightarrow [0, 1], \quad X_i \in 2^\Theta \quad (1)$$

If $m(X_i) > 0$, X_i is called the focal element. m_i denotes the mass assignments of the i th source of evidence. The Dempster's combination rule is given by [13,14]

$$m_{DS}(X) = \frac{\sum_{X_i \cap X_j = X, i \neq j} m_1(X_i) \cdot m_2(X_j)}{1 - K}, \quad \forall X \subseteq \Theta \quad (2)$$

$$K = \sum_{\substack{X_i, X_j \subseteq \Theta, i \neq j \\ X_i \cap X_j = \emptyset}} m_1(X_i) \cdot m_2(X_j) \quad (3)$$

where K denotes the conflict beliefs of evidences. However, when the conflict beliefs of evidences are high, the fusion results of Dempster's combination rule are usually very unreasonable. For this reason, many combination rules were developed, especially, Proportional Conflict Redistribution1–6 (PCR1–6) rules in DSMT framework have many advantages and successful applications [12].

2.2. Dezert–Smarandache theory (DSMT)

The discernment frame of DSMT based on the hyper-power set abandons the exclusiveness limitation of DST. The hyper-power set denoted by D^Θ admits the intersection of the elements. For example, if there are two elements in discernment framework $\Theta = \{\theta_1, \theta_2\}$, the hyper-power set is $D^\Theta = \{\emptyset, \theta_1, \theta_2, \theta_1 \cup \theta_2, \theta_1 \cap \theta_2\}$. The mass assignments of evidences defined over the hyper-power set D^Θ is defined by

$$m(X_i) : D^\Theta \rightarrow [0, 1], \quad X_i \in D^\Theta \quad (4)$$

The Proportional Conflict Redistribution (PCR) rules [41,42] are the combination rules in DSMT framework. PCR rules have PCR1–6 rules and the difference of them is that the proportional redistribution way of the conflict beliefs. PCR1–5 rules are applied for the combination of two sources and among these rules, PCR5 is considered as the most precise mathematical method. PCR6 rule is usually applied for more than two sources fusion problems.

PCR5 rule for 2 sources is introduced as follows [41,42]

$$m_{1 \oplus 2}(X_i) = \sum_{\substack{Y, Z \in G^\Theta \text{ and } Y, Z \neq \emptyset \\ Y \cap Z = X_i}} m_1(Y) \cdot m_2(Z) \quad (5)$$

$$m_{PCR5}(X_i) = \begin{cases} m_{1 \oplus 2}(X_i) \\ + \sum_{\substack{X_j \in G^\Theta \text{ and } i \neq j \\ X_i \cap X_j = \emptyset}} \left[\frac{m_1(X_i)^2 \cdot m_2(X_j)}{m_1(X_i) + m_2(X_j)} + \frac{m_2(X_i)^2 \cdot m_1(X_j)}{m_2(X_i) + m_1(X_j)} \right] \\ X_i \in G^\Theta \text{ and } X_i \neq \emptyset \\ 0, \quad X_i = \emptyset \end{cases} \quad (6)$$

where G^Θ can be seen as the power set 2^Θ , the hyper-power set D^Θ and the super-power set S^Θ , if discernment of the fusion problem satisfies the Shafer's model, the hybrid DSm model, and the minimal refinement Θ^{ref} of Θ respectively and where all denominators are more than zero and the fraction is discarded when the denominator of it is zero [41,42].

This paper is mainly for more than two sources fusion. PCR6 rule for more than 2 sources is introduced as follows

$$m_{1 \oplus 2 \oplus \dots \oplus s}(X) = \sum_{\substack{Y_1, Y_2, \dots, Y_s \in G^\Theta \text{ and } Y_1, Y_2, \dots, Y_s \neq \emptyset \\ Y_1 \cap Y_2 \cap \dots \cap Y_s = X}} m_1(Y_1) \times m_2(Y_2) \times \dots \times m_s(Y_s) \quad (7)$$

$$m_{ConflictTransfer}(X) = \sum_{\substack{Z_1, Z_2, \dots, Z_{s-1} \in G^\Theta \\ Z_i \neq X, i \in \{1, 2, \dots, s-1\} \\ (\bigcap_{i=1}^{s-1} Z_i) \cap X = \emptyset}} \sum_{k=1}^{s-1} \sum_{(i_1, i_2, \dots, i_s) \in P(1, 2, \dots, s)} [m_{i_1}(X) + m_{i_2}(X) + \dots + m_{i_k}(X)] \cdot \left[\frac{m_{i_1}(X) \times m_{i_2}(X) \times \dots \times m_{i_k}(X) \times m_{i_{k+1}}(Z_1) \times \dots \times m_{i_{k+1}}(Z_{s-k})}{m_{i_1}(X) + m_{i_2}(X) + \dots + m_{i_k}(X) + m_{i_{k+1}}(Z_1) + \dots + m_{i_{k+1}}(Z_{s-k})} \right] \quad (8)$$

$$m_{PCR6}(X) = m_{1 \oplus 2 \oplus \dots \oplus s}(X) + m_{ConflictTransfer}(X), \quad X \in G^\Theta \text{ and } X \neq \emptyset \quad (9)$$

where G^Θ denotes the general power set which can be seen as the same as 2^Θ , D^Θ or the super-power set S^Θ in different cases; and $P(1, 2, \dots, s)$ denotes the set of all permutations of the elements. Equation (7) denotes that the combination products of the intersections of the mass assignments. Equation (8) denotes that the proportional redistribution of the conflict beliefs of mass assignments.

Assume that $s = 2$, PCR6 rule is given by

$$m_{1 \oplus 2}(X) = \sum_{\substack{Y_1, Y_2 \in G^\Theta \text{ and } Y_1, Y_2 \neq \emptyset \\ Y_1 \cap Y_2 = X}} m_1(Y_1) \times m_2(Y_2) \quad (10)$$

$$m_{ConflictTransfer}(X) = m_{i_1}(X) \cdot \left[\frac{m_{i_1}(X) \times m_{i_2}(Z_2)}{m_{i_1}(X) + m_{i_2}(Z_2)} \right] + m_{i_2}(X) \cdot \left[\frac{m_{i_2}(X) \times m_{i_1}(Z_1)}{m_{i_2}(X) + m_{i_1}(Z_1)} \right] \quad (11)$$

$$m_{PCR6}(X) = \sum_{\substack{Y_1, Y_2 \in G^\Theta \text{ and } Y_1, Y_2 \neq \emptyset \\ Y_1 \cap Y_2 = X}} m_1(Y_1) \times m_2(Y_2) + m_{i_1}(X) \cdot \left[\frac{m_{i_1}(X) \times m_{i_2}(Z_2)}{m_{i_1}(X) + m_{i_2}(Z_2)} \right] + m_{i_2}(X) \cdot \left[\frac{m_{i_2}(X) \times m_{i_1}(Z_1)}{m_{i_2}(X) + m_{i_1}(Z_1)} \right], \quad X \in G^\Theta \text{ and } X \neq \emptyset \quad (12)$$

PCR has many advantages, such as it provides the appropriate re-distribution of conflicting beliefs, and it can produce reasonable combination result even in high conflicting cases. Nevertheless, the main disadvantage of PCR6 is that its computation complexity is too large and this limits its widely practical application.

2.3. Evidential distance theory

Evidential distance theory is a good way to measure the dissimilarity of multi evidences. Two well known dissimilarity measure functions based on evidential distance theory are introduced briefly; first is Jousselme dissimilarity measure function based on Jousselme’s distance which takes into account the cardinality of elements; second is Euclidean dissimilarity measure function which has little computation complexity and fast convergence speed.

1) Jousselme dissimilarity measure function $Sim_J(m_1, m_2)$ [37] is defined based on the Jousselme’s evidential distance [43] as follows

$$Sim_J(m_1, m_2) = 1 - \frac{1}{\sqrt{2}} \sqrt{(m_1 - m_2)^T D (m_1 - m_2)} \quad (13)$$

where $D = [D_{ij}]$ is a $|G^\Theta| \times |G^\Theta|$ positively definite matrix, and $D_{ij} = |X_i \cap X_j| / |X_i \cup X_j|$ with $X_i, X_j \in G^\Theta$.

The advantage of Jousselme dissimilarity is that it considers both the mass and the cardinality of bba’s. However, it makes no difference between the bba’s consisting of all single elements’ mass assignments and the bba’s consisting of non specific elements’ mass assignments [16].

2) Euclidean ESMS function $Sim_E(m_1, m_2)$ [37] is defined based on the Euclidean evidential distance as follows

$$Sim_E(m_1, m_2) = 1 - \frac{1}{\sqrt{2}} \sqrt{\sum_{i=1}^{|G^\Theta|} [m_1(X_i) - m_2(X_i)]^2} \quad (14)$$

where $|G^\Theta|$ is the cardinality of G^Θ .

The difference of $Sim_E(m_1, m_2)$ and $Sim_J(m_1, m_2)$ has been discussed in [37]. The detailed discussion is omitted in this paper. Please see [37] if necessary. It is proved in [37] that $Sim_E(m_1, m_2)$ has many properties, including fastest convergence speed. So it is adopted in this paper as the dissimilarity measure of the approximate method with DSmT + PCR6.

3. An evidence clustering DSmT approximate reasoning method for more than two sources

3.1. A new form of PCR6 formula for more than two sources

It can be drawn from Equation (5)–(7) that the fusion procedures of the PCR6 rule have two main steps, first is the calculation of $m_{1 \oplus 2 \oplus \dots \oplus s}(X)$ and second is the calculation of $m_{ConflictTransfer}(X)$. For reducing the computation complexity of our approximate reasoning method, a new form of the PCR6 formula for more than two sources is given as follows

1) The focal element of evidences from multi sources are denoted by

$$\begin{aligned} m_1 &: \{X_{i_1}^1\}, X_{i_1}^1 \in G^\Theta \\ m_2 &: \{X_{i_2}^2\}, X_{i_2}^2 \in G^\Theta \\ &\vdots \\ m_s &: \{X_{i_s}^s\}, X_{i_s}^s \in G^\Theta \end{aligned} \quad (15)$$

2) The first step fusion results of evidences are calculated by

$$\begin{aligned} m_{PCR-new}^1(X) &= m_{i_1}(X_{i_1}^1) \\ &\cdot \sum_{X_{i_2}^2, X_{i_3}^3, \dots, X_{i_s}^s \in G^\Theta} \left[\frac{m_{i_1}(X_{i_1}^1) \times m_{i_2}(X_{i_2}^2) \times \dots \times m_{i_s}(X_{i_s}^s)}{m_{i_1}(X_{i_1}^1) + m_{i_2}(X_{i_2}^2) + \dots + m_{i_s}(X_{i_s}^s)} \right], \\ \text{if } X_{i_1}^1 \cap X_{i_2}^2 \cap \dots \cap X_{i_s}^s &= \emptyset, X = X_{i_1}^1, \\ \text{else } X &= X_{i_1}^1 \cap X_{i_2}^2 \cap \dots \cap X_{i_s}^s \\ m_{PCR-new}^2(X) &= m_{i_2}(X_{i_2}^2) \\ &\cdot \sum_{X_{i_1}^1, X_{i_3}^3, \dots, X_{i_s}^s \in G^\Theta} \left[\frac{m_{i_1}(X_{i_1}^1) \times m_{i_2}(X_{i_2}^2) \times \dots \times m_{i_s}(X_{i_s}^s)}{m_{i_1}(X_{i_1}^1) + m_{i_2}(X_{i_2}^2) + \dots + m_{i_s}(X_{i_s}^s)} \right], \\ \text{if } X_{i_2}^2 \cap X_{i_1}^1 \cap \dots \cap X_{i_s}^s &= \emptyset, X = X_{i_2}^2, \\ \text{else } X &= X_{i_2}^2 \cap X_{i_1}^1 \cap \dots \cap X_{i_s}^s \\ &\vdots \\ m_{PCR-new}^s(X) &= m_{i_s}(X_{i_s}^s) \\ &\cdot \sum_{X_{i_1}^1, X_{i_2}^2, \dots, X_{i_{s-1}}^{s-1} \in G^\Theta} \left[\frac{m_{i_1}(X_{i_1}^1) \times m_{i_2}(X_{i_2}^2) \times \dots \times m_{i_s}(X_{i_s}^s)}{m_{i_1}(X_{i_1}^1) + m_{i_2}(X_{i_2}^2) + \dots + m_{i_s}(X_{i_s}^s)} \right], \\ \text{if } X_{i_s}^s \cap X_{i_1}^1 \cap \dots \cap X_{i_{s-1}}^{s-1} &= \emptyset, X = X_{i_s}^s, \\ \text{else } X &= X_{i_s}^s \cap X_{i_1}^1 \cap \dots \cap X_{i_{s-1}}^{s-1} \end{aligned} \quad (16)$$

3) The final fusion results are calculated by

$$m_{PCR-new}(X) = m_{PCR-new}^1(X) + m_{PCR-new}^2(X) + \dots + m_{PCR-new}^s(X) \quad (17)$$

3.2. Mathematical analysis of new form of PCR6 formula

It can be drawn from Equation (16) that $m_{PCR-new}^1(X), m_{PCR-new}^2(X), \dots, m_{PCR-new}^s(X)$ have the similar formula form. Due to the similar formula form, $m_{PCR-new}^1(X)$ is analyzed first.

$$\begin{aligned} m_{PCR-new}^1(X) &= m_{i_1}(X_{i_1}^1) \\ &\cdot \sum_{X_{i_2}^2, X_{i_3}^3, \dots, X_{i_s}^s \in G^\Theta} \left[\frac{m_{i_1}(X_{i_1}^1) \times m_{i_2}(X_{i_2}^2) \times \dots \times m_{i_s}(X_{i_s}^s)}{m_{i_1}(X_{i_1}^1) + m_{i_2}(X_{i_2}^2) + \dots + m_{i_s}(X_{i_s}^s)} \right] \\ &= m_{i_1}(X_{i_1}^1)^2 \times \sum_{X_{i_3}^3, \dots, X_{i_s}^s \in G^\Theta} \left\{ m_{i_3}(X_{i_3}^3) \times \dots \times m_{i_s}(X_{i_s}^s) \right. \\ &\quad \left. \times \sum_{X_{i_2}^2 \in G^\Theta} \left[\frac{m_{i_2}(X_{i_2}^2)}{m_{i_1}(X_{i_1}^1) + m_{i_2}(X_{i_2}^2) + \dots + m_{i_s}(X_{i_s}^s)} \right] \right\} \end{aligned} \quad (18)$$

Let

$$\begin{aligned} m_{i_1}(X_{i_1}^1) + m_{i_3}(X_{i_3}^3) + \dots + m_{i_s}(X_{i_s}^s) &= a, \\ m_{i_2}(X_{i_2}^2) &= x_1, x_2, \dots, x_n. \end{aligned} \quad (19)$$

Then

$$\begin{aligned} & \sum_{X_{i_2}^2 \in G^\Theta} \left[\frac{m_{i_2}(X_{i_2}^2)}{m_{i_1}(X_{i_1}^1) + m_{i_2}(X_{i_2}^2) + \dots + m_{i_s}(X_{i_s}^s)} \right] \\ &= \frac{x_1}{a+x_1} + \frac{x_2}{a+x_2} + \dots + \frac{x_n}{a+x_n} \\ &= n - a \times \left(\frac{1}{a+x_1} + \frac{1}{a+x_2} + \dots + \frac{1}{a+x_n} \right) \end{aligned} \quad (20)$$

Let

$$f(x_i) = \frac{1}{a+x_i}, \quad i = 1, 2, \dots, n, \quad 0 \leq x_i \leq 1. \quad (21)$$

Because $f(x_i)$ is a convex function, the approximate convex function formula [44] of $\sum_{i=1}^n f(x_i)$ is given by

$$\begin{aligned} \sum_{i=1}^n f(x_i) &= \frac{1}{a+x_1} + \frac{1}{a+x_2} + \dots + \frac{1}{a+x_n} \\ &= \frac{n}{a+(x_1+x_2+\dots+x_n)/n} + \Delta \end{aligned} \quad (22)$$

where Δ denotes the error of the approximate convex function formula, $\Delta \geq 0$, $\Delta = 0$ iff $x_1 = x_2 = \dots = x_n$. Let $x_0 = (x_1 + x_2 + \dots + x_n)/n$, the convex function error analysis can be seen in [44] and the convex error function formula is given by

$$\Delta \approx \frac{\sum_{i=1}^n (x_i - x_0)^2}{2(a+x_0)^3}, \quad x_i < a + 2x_0 \quad (23)$$

From Equation (23), the convex function errors are related to $\sum_{i=1}^n (x_i - x_0)^2$ and $\frac{1}{2(a+x_0)^3}$. If the average value x_0 is large and x_1, x_2, \dots, x_n are concentrated, the errors are much smaller.

Let n is the number of focal elements in the evidence, j is the source order number, $j = 1, 2, \dots, s$ and $\{x_i^j\}$, $i = 1, 2, \dots, n$ are the bba's of the j th source's evidence.

The pseudo-code of Evidence Clustering method is given as Table 1.

Table 1
The pseudo-code of Evidence Clustering method.

Input:	
The number of focal elements in the evidence: n	
The source order number: $j = 1, 2, \dots, s$	
The bba's of the j th source's evidence: $\{x_i^j\}$, $i = 1, 2, \dots, n$	
1) For $j = 1, 2, \dots, s$	
$\{x_i^j\}$, $i = 1, 2, \dots, n$ are reordered to be $\{x_i^j\}$, $x_1^j \geq x_2^j \geq \dots \geq x_n^j$ in descending order.	
End	
2) For $i = 1, 2, \dots, n$	
Calculate the following function	
$f(x_i^j) = \frac{1.5 \cdot (1 - \sum_{k=1}^i x_k^j)}{n - i} \quad (24)$	
If $x_i^j \geq f(x_i^j)$, x_i^j is forced to the set x_a^j .	
Otherwise, x_i^j and the following mass assignments are forced to the other set x_b^j .	
End	
3) For $j = 1, 2, \dots, s$	
Calculate the sum and the number of x_a^j .	
The sum of x_a^j is denoted by X_a^j and the number of x_a^j is denoted by k_a^j .	
Then the sum of x_b^j is denoted by $X_b^j = 1 - X_a^j$, the number of x_b^j is denoted by $k_b^j = n - k_a^j$.	
End	

After the above Evidence Clustering method, the mass assignments are clustered to two sets, denoted by x_a^j and x_b^j . Besides, the sum and the number of two sets is calculated.

Based on the Evidence Clustering method and the approximate convex function formula, Equation (16) can be transferred to

$$\begin{aligned} & m_{\text{PCR-new}}^1(X) \\ &= m_{i_1}(X_{i_1}^1)^2 \sum_{X_{i_3}^3, \dots, X_{i_s}^s \in G^\Theta} \left\{ m_{i_3}(X_{i_3}^3) \times \dots \times m_{i_s}(X_{i_s}^s) \right. \\ & \quad \left. \times \sum_{X_{i_2}^2 \in G^\Theta} \left[\frac{m_{i_2}(X_{i_2}^2)}{m_{i_1}(X_{i_1}^1) + m_{i_2}(X_{i_2}^2) + \dots + m_{i_s}(X_{i_s}^s)} \right] \right\} \\ & \approx m_{i_1}(X_{i_1}^1)^2 \sum_{X_{i_3}^3, \dots, X_{i_s}^s \in G^\Theta} \left\{ m_{i_3}(X_{i_3}^3) \times \dots \times m_{i_s}(X_{i_s}^s) \right. \\ & \quad \left. \times \left[\frac{X_a^2}{m_{i_1}(X_{i_1}^1) + m_{i_3}(X_{i_3}^3) + \dots + m_{i_s}(X_{i_s}^s) + X_a^2/k_a^2} \right. \right. \\ & \quad \left. \left. + \frac{X_b^2}{m_{i_1}(X_{i_1}^1) + m_{i_3}(X_{i_3}^3) + \dots + m_{i_s}(X_{i_s}^s) + X_b^2/k_b^2} \right] \right\} \\ &= m_{i_1}(X_{i_1}^1)^2 \sum_{X_{i_4}^4, \dots, X_{i_s}^s \in G^\Theta} \left\{ m_{i_4}(X_{i_4}^4) \times \dots \times m_{i_s}(X_{i_s}^s) \right. \\ & \quad \left. \times \sum_{X_{i_3}^3 \in G^\Theta} m_{i_3}(X_{i_3}^3) \left[\frac{X_a^2}{m_{i_1}(X_{i_1}^1) + m_{i_3}(X_{i_3}^3) + \dots + m_{i_s}(X_{i_s}^s) + X_a^2/k_a^2} \right. \right. \\ & \quad \left. \left. + \frac{X_b^2}{m_{i_1}(X_{i_1}^1) + m_{i_3}(X_{i_3}^3) + \dots + m_{i_s}(X_{i_s}^s) + X_b^2/k_b^2} \right] \right\} \end{aligned} \quad (25)$$

Let

$$\begin{aligned} & m_{i_1}(X_{i_1}^1) + m_{i_4}(X_{i_4}^4) + \dots + m_{i_s}(X_{i_s}^s) + X_a^2/k_a^2 = a, \\ & m_{i_3}(X_{i_3}^3) = x_1, x_2, \dots, x_n. \end{aligned} \quad (26)$$

Then

$$\begin{aligned} & \sum_{X_{i_3}^3 \in G^\Theta} m_{i_3}(X_{i_3}^3) \cdot \frac{X_a^2}{m_{i_1}(X_{i_1}^1) + m_{i_3}(X_{i_3}^3) + \dots + m_{i_s}(X_{i_s}^s) + X_a^2/k_a^2} \\ &= X_a^2 \times \left[\frac{x_1}{a+x_1} + \frac{x_2}{a+x_2} + \dots + \frac{x_n}{a+x_n} \right] \end{aligned} \quad (27)$$

Based on the Evidence Clustering method and the approximate convex function formula, Equation (27) can be transferred to

$$\begin{aligned} & \sum_{X_{i_3}^3 \in G^\Theta} m_{i_3}(X_{i_3}^3) \cdot \frac{X_a^2}{m_{i_1}(X_{i_1}^1) + m_{i_3}(X_{i_3}^3) + \dots + m_{i_s}(X_{i_s}^s) + X_a^2/k_a^2} \\ &= X_a^2 \times \frac{X_a^3}{m_{i_1}(X_{i_1}^1) + X_a^2/k_a^2 + X_a^3/k_a^3 + m_{i_4}(X_{i_4}^4) + \dots + m_{i_s}(X_{i_s}^s)} \end{aligned} \quad (28)$$

Then Equation (16) can be transferred to

$$\begin{aligned} & m_{\text{PCR-new}}^1(X) \\ &= m_{i_1}(X_{i_1}^1)^2 \sum_{X_{i_4}^4, \dots, X_{i_s}^s \in G^\Theta} \left\{ m_{i_4}(X_{i_4}^4) \times \dots \times m_{i_s}(X_{i_s}^s) \right. \end{aligned}$$

$$\times \left[\begin{array}{l} X_a^2 \times \frac{X_a^3}{m_{i_1}(X_{i_1}^1) + X_a^3/k_a^3 + X_a^2/k_a^2 + m_{i_4}(X_{i_4}^4) + \dots + m_{i_s}(X_{i_s}^s)} \\ + X_a^2 \times \frac{X_b^3}{m_{i_1}(X_{i_1}^1) + X_b^3/k_b^3 + X_a^2/k_a^2 + m_{i_4}(X_{i_4}^4) + \dots + m_{i_s}(X_{i_s}^s)} \\ + X_b^2 \times \frac{X_a^3}{m_{i_1}(X_{i_1}^1) + X_a^3/k_a^3 + X_b^2/k_b^2 + m_{i_4}(X_{i_4}^4) + \dots + m_{i_s}(X_{i_s}^s)} \\ + X_b^2 \times \frac{X_b^3}{m_{i_1}(X_{i_1}^1) + X_b^3/k_b^3 + X_b^2/k_b^2 + m_{i_4}(X_{i_4}^4) + \dots + m_{i_s}(X_{i_s}^s)} \end{array} \right] \quad (29)$$

Equation (29) can be transformed to the products of the sum of convex functions. So the mass assignments of focal elements are clustered by Evidence Clustering method for reducing the approximate errors and the approximate formula of Equation (16) is given as follows

$$\begin{aligned} m_{\text{PCR-new}}^1(X) &\approx m_{\text{PCR-CONVEX}}^1(X) \\ &= m_{i_1}(X_{i_1}^1)^2 \\ &\times \sum_{\substack{t^2 \in \{X_a^2, X_b^2\}, k^2 \in \{k_a^2, k_b^2\} \\ t^3 \in \{X_a^3, X_b^3\}, k^3 \in \{k_a^3, k_b^3\} \\ \vdots \\ t^s \in \{X_a^s, X_b^s\}, k^s \in \{k_a^s, k_b^s\}}} \frac{t^2 \times t^3 \times \dots \times t^s}{m_{i_1}(X_{i_1}^1) + t^2/k^2 + t^3/k^3 + \dots + t^s/k^s} \end{aligned} \quad (30)$$

where if $t^j = X_a^j$, $k^j = k_a^j$ and if $t^j = X_b^j$, $k^j = k_b^j$.

Similarly, the approximate formulas of $m_{\text{PCR-new}}^j(X)$, $j = 1, 2, \dots, s$ in Equation (16) are given as follows

$$\begin{aligned} m_{\text{PCR-CONVEX}}^j(X) &= m_{i_j}(X_{i_j}^j)^2 \\ &\cdot \sum_{l \neq j, l \in \{1, 2, \dots, s\}} \left[\frac{\prod_{l \neq j, l \in \{1, 2, \dots, s\}} m_{i_l}(X_{i_l}^l)}{m_{i_j}(X_{i_j}^j) + \sum_{l \neq j, l \in \{1, 2, \dots, s\}} m_{i_l}(X_{i_l}^l)} \right] \\ &= m_{i_j}(X_{i_j}^j)^2 \\ &\times \sum_{\substack{t^l \in \{X_a^l, X_b^l\}, k^l \in \{k_a^l, k_b^l\} \\ k^l = k_a^l, \text{ if } t^l = X_a^l \\ k^l = k_b^l, \text{ if } t^l = X_b^l}} \frac{\prod_{l \neq j, l \in \{1, 2, \dots, s\}} t^l}{m_{i_j}(X_{i_j}^j) + \sum_{l \neq j, l \in \{1, 2, \dots, s\}} t^l/k^l} \end{aligned} \quad (31)$$

The Approximate Reasoning method is given as Table 2.

3.3. Analysis of computation complexity

Assume that s denotes the number of multi sources, and $s > 2$; n denotes the number of singleton focal elements in each evidence; there are only mass assignments of singleton focal elements in multi source evidences, denoted by $m(\theta_i) > 0 | \theta_i \in G^\Theta = \{\theta_1, \theta_2, \dots, \theta_n\}$; M, A, and D denote the computation complexity of multiplication, addition, and division for one time, separately.

The computation complexity of PCR6 for more than two sources, denoted by $o_{\text{PCR6}}(n, s)$ is given by

$$o_{\text{PCR6}}(n, s) = n \cdot (s - 1) \cdot M + s \cdot (n^s - n) \cdot [s \cdot M + (s - 1) \cdot A + D] + n \cdot A$$

Table 2

The pseudo-code of approximate reasoning method.

Input: The number of focal elements in the evidence: n
The source order number: $j = 1, 2, \dots, s$
The bba's of the j th source's evidence: $\{x_i^j\}$, $i = 1, 2, \dots, n$
the sum and the number of the two clustering sets of $\{x_i^j\}$: X_a^j, k_a^j and X_b^j, k_b^j
1) For $j = 1, 2, \dots, s$
Calculate the following function

$$\begin{aligned} m_{\text{PCR-CONVEX}}^j(X) &= m_{i_j}(X_{i_j}^j)^2 \\ &\times \sum_{\substack{t^l \in \{X_a^l, X_b^l\}, k^l \in \{k_a^l, k_b^l\} \\ k^l = k_a^l, \text{ if } t^l = X_a^l \\ k^l = k_b^l, \text{ if } t^l = X_b^l}} \frac{\prod_{l \neq j, l \in \{1, 2, \dots, s\}} t^l}{m_{i_j}(X_{i_j}^j) + \sum_{l \neq j, l \in \{1, 2, \dots, s\}} t^l/k^l} \end{aligned} \quad (32)$$

End

Calculate the convex approximate formula of Equation (17) as follows

$$m_{\text{CONVEX}}(X) = m_{\text{PCR-CONVEX}}^1(X) + m_{\text{PCR-CONVEX}}^2(X) + \dots + m_{\text{PCR-CONVEX}}^s(X) \quad (33)$$

Calculate the final approximate results by the normalization step as follows

$$m_{\text{GH}}(X) = \frac{m_{\text{CONVEX}}(X)}{\sum_{X \in G^\Theta} m_{\text{CONVEX}}(X)} \quad (34)$$

$$\begin{aligned} &= [n \cdot (s - 1) + s^2 \cdot n \cdot (n^{s-1} - 1)] \cdot M \\ &+ [s \cdot (n^s - n) \cdot (s - 1) + n] \cdot A + s \cdot (n^s - n) \cdot D \end{aligned} \quad (35)$$

Proof. Assume that the multisource evidences are shown as follows:

$$\begin{array}{ccccccc} m_1(\theta_1) & m_1(\theta_2) & \dots & m_1(\theta_n) \\ m_2(\theta_1) & m_2(\theta_2) & \dots & m_2(\theta_n) \\ \vdots & & & \\ m_s(\theta_1) & m_s(\theta_2) & \dots & m_s(\theta_n) \end{array} \quad (36)$$

The original PCR6 method can be divided into two parts as Equation (5), Equation (6) and Equation (7).

1) First, the computation of Equation (5) can be represented by $m_{1 \oplus 2 \oplus \dots \oplus s}(\theta_i) = m_1(\theta_i) \times m_2(\theta_i) \times \dots \times m_s(\theta_i)$ (37)

The computation of Equation (37) consists of $(s - 1)$ times of multiplication, denoted by $(s - 1) \cdot M$.

Because $i = 1, 2, \dots, n$, the computation complexity of Equation (5) of PCR6 method can be drawn as follows

$$o_{\text{PCR6-Equation (5)}}(n, s) = n \cdot (s - 1) \cdot M. \quad (38)$$

2) Then the computation of Equation (6) can be represented by

$$\begin{aligned} m_{\text{ConflictTransfer}}(\theta_i) &= \sum_{\substack{Y_1, Y_2, \dots, Y_{s-1} \in G^\Theta \\ (\bigcap_{i=1}^{s-1} Y_i) \cap \theta_i = \emptyset}} m_1(\theta_i) \\ &\times \frac{m_1(\theta_i) \times m_2(Y_1) \times \dots \times m_s(Y_{s-1})}{m_1(\theta_i) + m_2(Y_1) + \dots + m_s(Y_{s-1})} \\ &+ \sum_{\substack{Y_1, Y_2, \dots, Y_{s-1} \in G^\Theta \\ (\bigcap_{i=1}^{s-1} Y_i) \cap \theta_i = \emptyset}} m_2(\theta_i) \\ &\times \frac{m_2(\theta_i) \times m_1(Y_1) \times \dots \times m_s(Y_{s-1})}{m_2(\theta_i) + m_1(Y_1) + \dots + m_s(Y_{s-1})} \end{aligned}$$

$$\begin{aligned}
& + \cdots + \sum_{\substack{Y_1, Y_2, \dots, Y_{s-1} \in G^\Theta \\ (\bigcap_{i=1}^{s-1} Y_i) \cap \theta_i = \emptyset}} m_s(\theta_i) \\
& \times \frac{m_s(\theta_i) \times m_1(Y_1) \times \cdots \times m_{s-1}(Y_{s-1})}{m_s(\theta_i) + m_1(Y_1) + \cdots + m_{s-1}(Y_{s-1})} \\
= & \sum_{Y_1, Y_2, \dots, Y_{s-1} \in G^\Theta} m_1(\theta_i) \\
& \times \frac{m_1(\theta_i) \times m_2(Y_1) \times \cdots \times m_s(Y_{s-1})}{m_1(\theta_i) + m_2(Y_1) + \cdots + m_s(Y_{s-1})} - m_1(\theta_i) \\
& \times \frac{m_1(\theta_i) \times m_2(\theta_i) \times \cdots \times m_s(\theta_i)}{m_1(\theta_i) + m_2(\theta_i) + \cdots + m_s(\theta_i)} \\
& + \sum_{Y_1, Y_2, \dots, Y_{s-1} \in G^\Theta} m_2(\theta_i) \\
& \times \frac{m_2(\theta_i) \times m_1(Y_1) \times \cdots \times m_s(Y_{s-1})}{m_2(\theta_i) + m_1(Y_1) + \cdots + m_s(Y_{s-1})} - m_2(\theta_i) \\
& \times \frac{m_2(\theta_i) \times m_1(\theta_i) \times \cdots \times m_s(\theta_i)}{m_2(\theta_i) + m_1(\theta_i) + \cdots + m_s(\theta_i)} \\
& + \vdots \\
& + \sum_{Y_1, Y_2, \dots, Y_{s-1} \in G^\Theta} m_s(\theta_i) \\
& \times \frac{m_s(\theta_i) \times m_1(Y_1) \times \cdots \times m_{s-1}(Y_{s-1})}{m_s(\theta_i) + m_1(Y_1) + \cdots + m_{s-1}(Y_{s-1})} - m_s(\theta_i) \\
& \times \frac{m_s(\theta_i) \times m_1(\theta_i) \times \cdots \times m_{s-1}(\theta_i)}{m_s(\theta_i) + m_1(\theta_i) + \cdots + m_{s-1}(\theta_i)} \quad (39)
\end{aligned}$$

One part of the Equation (39) is analyzed as follows

$$\begin{aligned}
& \sum_{Y_1, Y_2, \dots, Y_{s-1} \in G^\Theta} m_1(\theta_i) \times \frac{m_1(\theta_i) \times m_2(Y_1) \times \cdots \times m_s(Y_{s-1})}{m_1(\theta_i) + m_2(Y_1) + \cdots + m_s(Y_{s-1})} \\
& - m_1(\theta_i) \times \frac{m_1(\theta_i) \times m_2(\theta_i) \times \cdots \times m_s(\theta_i)}{m_1(\theta_i) + m_2(\theta_i) + \cdots + m_s(\theta_i)} \quad (40)
\end{aligned}$$

The computation of Equation (40) consists of $(n^{s-1} - 1) \cdot s$ times of multiplication, denoted by $(n^{s-1} - 1) \cdot s \cdot M$; $(n^{s-1} - 1) \cdot (s - 1)$ times of addition, denoted by $(n^{s-1} - 1) \cdot (s - 1) \cdot A$; and $(n^{s-1} - 1)$ times of division, denoted by $(n^{s-1} - 1) \cdot D$.

So the computation complexity of Equation (39) can be represented by $s \cdot (n^{s-1} - 1) \cdot [s \cdot M + (s - 1) \cdot A + D]$.

Because $i = 1, 2, \dots, n$, the computation complexity of Equation (6) of PCR6 method can be drawn as follows

$$O_{\text{PCR6-Equation (6)}}(n, s) = s \cdot (n^s - n) \cdot [s \cdot M + (s - 1) \cdot A + D]. \quad (41)$$

3) Thirdly the computation of Equation (7) can be represented by

$$m_{\text{PCR6}}(\theta_i) = m_{1 \oplus 2 \oplus \dots \oplus s}(\theta_i) + m_{\text{ConflictTransfer}}(\theta_i) \quad (42)$$

Because $i = 1, 2, \dots, n$, the computation complexity of Equation (7) of PCR6 method can be drawn as follows

$$O_{\text{PCR6-Equation (7)}}(n, s) = n \cdot A \quad (43)$$

Based on the above proof, the computation complexity of PCR6 method can be drawn as follows

$$\begin{aligned}
O_{\text{PCR6}}(n, s) \\
= & O_{\text{PCR6-Equation (5)}}(n, s) + O_{\text{PCR6-Equation (6)}}(n, s) \\
& + O_{\text{PCR6-Equation (7)}}(n, s)
\end{aligned}$$

$$\begin{aligned}
& = n \cdot (s - 1) \cdot M + s \cdot (n^s - n) \cdot [s \cdot M + (s - 1) \cdot A + D] + n \cdot A \\
& = [n \cdot (s - 1) + s^2 \cdot n \cdot (n^{s-1} - 1)] \cdot M \\
& \quad + [s \cdot (n^s - n) \cdot (s - 1) + n] \cdot A + s \cdot (n^s - n) \cdot D \quad \square \quad (44)
\end{aligned}$$

The computation complexity of the method in this paper, denoted by $O_{\text{GH}}(n, s)$, is given as follows

$$\begin{aligned}
O_{\text{GH}}(n, s) \\
= & s \cdot n \cdot 2^{s-1} \cdot [s \cdot M + (s - 1) \cdot A + s \cdot D] \\
& + n \cdot (s - 1) \cdot A + (n - 1) \cdot A + n \cdot D \\
= & s^2 \cdot n \cdot 2^{s-1} \cdot M + [s \cdot n \cdot 2^{s-1} \cdot (s - 1) + s \cdot n - 1] \cdot A \\
& + (s^2 \cdot n \cdot 2^{s-1} + n) \cdot D \quad (45)
\end{aligned}$$

Proof. Assume that the multisource evidences are shown as follows:

$$\begin{array}{cccc}
m_1(\theta_1) & m_1(\theta_2) & \cdots & m_1(\theta_n) \\
m_2(\theta_1) & m_2(\theta_2) & \cdots & m_2(\theta_n) \\
\vdots & \vdots & \vdots & \vdots \\
m_s(\theta_1) & m_s(\theta_2) & \cdots & m_s(\theta_n)
\end{array} \quad (46)$$

Each evidence is clustered by Evidence Clustering method and two sets of each evidence are generated. The sum and the number of two sets (sum, number) is obtained as follows

$$\begin{array}{cc}
(X_a^1, k_a^1) & (X_b^1, k_b^1) \\
(X_a^2, k_a^2) & (X_b^2, k_b^2) \\
\vdots & \vdots \\
(X_a^s, k_a^s) & (X_b^s, k_b^s)
\end{array} \quad (47)$$

The proposed method in this paper consists of Equation (32) to Equation (34).

1) The computation of Equation (32) when $j = 1$ can be represented by

$$\begin{aligned}
m_{\text{PCR-new}}^1(\theta_i) \\
= & m_1(\theta_i)^2 \\
& \times \sum_{\substack{t^2 \in \{X_a^2, X_b^2\}, k^2 \in \{k_a^2, k_b^2\} \\ t^3 \in \{X_a^3, X_b^3\}, k^3 \in \{k_a^3, k_b^3\} \\ \vdots \\ t^s \in \{X_a^s, X_b^s\}, k^s \in \{k_a^s, k_b^s\}}} \frac{t^2 \times t^3 \times \cdots \times t^s}{m_1(\theta_i) + t^2/k^2 + t^3/k^3 + \cdots + t^s/k^s} \quad (48)
\end{aligned}$$

where if $t^j = X_a^j$, $k^j = k_a^j$ and if $t^j = X_b^j$, $k^j = k_b^j$.

Because each of t^2, t^3, \dots, t^s has 2 possibilities,

$$\sum_{\substack{t^2 \in \{X_a^2, X_b^2\}, k^2 \in \{k_a^2, k_b^2\} \\ t^3 \in \{X_a^3, X_b^3\}, k^3 \in \{k_a^3, k_b^3\} \\ \vdots \\ t^s \in \{X_a^s, X_b^s\}, k^s \in \{k_a^s, k_b^s\}}} \frac{t^2 \times t^3 \times \cdots \times t^s}{m_1(\theta_i) + t^2/k^2 + t^3/k^3 + \cdots + t^s/k^s}$$

has 2^{s-1} items.

Because $i = 1, 2, \dots, n$, the computation complexity of Equation (32) when $j = 1$ can be drawn as follows

$$O_{\text{GH-Equation (32-j=1)}}(n, s) = n \cdot 2^{s-1} \cdot [s \cdot M + (s - 1) \cdot A + s \cdot D] \quad (49)$$

Table 3

The numerical examples of computation complexity comparison.

The increment of numbers of sources	The method	Numbers of division	Numbers of addition	Numbers of multiplications
10	PCR6 method	1×10^{11}	9×10^{11}	1×10^{12}
	The proposed method	10240	92250	102400
50	PCR6 method	5×10^{51}	2.45×10^{53}	2.5×10^{53}
	The proposed method	5.63×10^{16}	2.76×10^{18}	2.81×10^{18}
100	PCR6 method	1×10^{102}	9.9×10^{103}	1×10^{104}
	The proposed method	1.27×10^{32}	1.26×10^{34}	1.27×10^{34}
200	PCR6 method	2×10^{202}	3.98×10^{204}	4×10^{204}
	The proposed method	3.21×10^{62}	6.40×10^{64}	6.43×10^{64}

2) Because Equation (32) when $j = 1, 2, \dots, s$ has symmetry, the computation complexity of Equation (32) can be drawn as follows

$$O_{\text{GH-Equation (32)}}(n, s) = s \cdot n \cdot 2^{s-1} \cdot [s \cdot M + (s-1) \cdot A + s \cdot D] \quad (50)$$

3) The computation of Equation (33) can be represented by

$$O_{\text{GH-Equation (33)}}(n, s) = n \cdot (s-1) \cdot A \quad (51)$$

4) The computation of Equation (34) can be represented by

$$O_{\text{GH-Equation (34)}}(n, s) = (n-1) \cdot A + n \cdot D \quad (52)$$

Based on the above proof, the computation complexity of the proposed method can be drawn as follows

$$\begin{aligned} O_{\text{GH}}(n, s) &= s \cdot n \cdot 2^{s-1} \cdot [s \cdot M + (s-1) \cdot A + s \cdot D] \\ &\quad + n \cdot (s-1) \cdot A + (n-1) \cdot A + n \cdot D \\ &= s^2 \cdot n \cdot 2^{s-1} \cdot M + [s \cdot n \cdot 2^{s-1} \cdot (s-1) + s \cdot n - 1] \cdot A \\ &\quad + (s^2 \cdot n \cdot 2^{s-1} + n) \cdot D \quad \square \end{aligned} \quad (53)$$

It can be drawn from Equation (35) and Equation (45) that the computation complexity of PCR6 is almost proportion to $s^2 \cdot n^s$ and the computation complexity of the method in this paper is almost proportion to $s^2 \cdot 2^s$. Analysis of computation complexity show that the method in this paper cost much less computation complexity than DSMT + PCR6, especially when the number of sources and the focal elements is large.

Although the above theoretical analysis shows that the proposed method has higher computational efficiency than the original PCR6 method, the numerical examples are also given to verify this conclusion. Assume that there are only 10 singleton focal elements which have mass assignments in hyper-power sets, denoted by $G^\ominus = \{\theta_1, \theta_2, \dots, \theta_{10}\}$. The numbers of division, numbers of addition and numbers of multiplications based on PCR6 method and the proposed method with the increment of numbers of sources are shown as Table 3. It can be drawn that the proposed method has more higher computational efficiency than the original PCR6 method especially when the number of sources is large.

4. Simulation experiments

4.1. Simple cases of only singleton focal elements

Example 1. If there are 3 evidence sources, assume that only singleton focal elements have mass assignments in hyper-power sets, denoted by $G_k^\ominus = \{\theta_1, \theta_2, \dots, \theta_5\}$, $k = 1, 2, 3$. The mass assignments in each evidence are $\mathbf{m}^1 = \{0.1, 0.1, 0.3, 0.3, 0.2\}$, $\mathbf{m}^2 = \{0.2, 0.3, 0.05, 0.3, 0.15\}$, $\mathbf{m}^3 = \{0.1, 0.05, 0.4, 0.35, 0.1\}$.

1) The mass assignments of focal elements in each evidence are clustered to two sets by the Evidence Clustering method, denoted by $x_a^1 = \{\theta_3, \theta_4, \theta_5\}$, $x_b^1 = \{\theta_1, \theta_2\}$; $x_a^2 = \{\theta_1, \theta_2, \theta_4, \theta_5\}$, $x_b^2 = \{\theta_3\}$; $x_a^3 = \{\theta_4, \theta_5\}$, $x_b^3 = \{\theta_1, \theta_2, \theta_3\}$.

Then

$$\begin{aligned} X_a^1 &= m_3^1(\theta_3) + m_4^1(\theta_4) + m_5^1(\theta_5) = 0.8 \\ X_b^1 &= m_1^1(\theta_1) + m_2^1(\theta_2) = 0.2 \\ X_a^2 &= m_1^2(\theta_1) + m_2^2(\theta_2) + m_4^2(\theta_4) + m_5^2(\theta_5) = 0.95 \\ X_b^2 &= m_3^2(\theta_3) = 0.05 \\ X_a^3 &= m_4^3(\theta_4) + m_5^3(\theta_5) = 0.75 \\ X_b^3 &= m_1^3(\theta_1) + m_2^3(\theta_2) + m_3^3(\theta_3) = 0.25 \end{aligned} \quad (54)$$

2) The convex function approximate fusion results are calculated by Equation (32)

$$\begin{aligned} m_{\text{PCR-CONVEX}}^1(\theta_1) &= \frac{m_1^1(\theta_1)^2 \cdot X_a^2 \cdot X_a^3}{m_1^1(\theta_1) + X_a^2/3 + X_a^3/2} + \frac{m_1^1(\theta_1)^2 \cdot X_a^2 \cdot X_b^3}{m_1^1(\theta_1) + X_a^2/3 + X_b^3/3} \\ &\quad + \frac{m_1^1(\theta_1)^2 \cdot X_b^2 \cdot X_b^3}{m_1^1(\theta_1) + X_b^2/2 + X_b^3/3} + \frac{m_1^1(\theta_1)^2 \cdot X_b^2 \cdot X_a^3}{m_1^1(\theta_1) + X_b^2/2 + X_a^3/2} \\ &= 0.0169 \\ m_{\text{PCR-CONVEX}}^1(\theta_2) &= \frac{m_2^1(\theta_2)^2 \cdot X_a^2 \cdot X_a^3}{m_2^1(\theta_2) + X_a^2/3 + X_a^3/2} + \frac{m_2^1(\theta_2)^2 \cdot X_a^2 \cdot X_b^3}{m_2^1(\theta_2) + X_a^2/3 + X_b^3/3} \\ &\quad + \frac{m_2^1(\theta_2)^2 \cdot X_b^2 \cdot X_b^3}{m_2^1(\theta_2) + X_b^2/2 + X_b^3/3} + \frac{m_2^1(\theta_2)^2 \cdot X_b^2 \cdot X_a^3}{m_2^1(\theta_2) + X_b^2/2 + X_a^3/2} \\ &= 0.0169 \\ m_{\text{PCR-CONVEX}}^1(\theta_3) &= \frac{m_3^1(\theta_3)^2 \cdot X_a^2 \cdot X_a^3}{m_3^1(\theta_3) + X_a^2/3 + X_a^3/2} + \frac{m_3^1(\theta_3)^2 \cdot X_a^2 \cdot X_b^3}{m_3^1(\theta_3) + X_a^2/3 + X_b^3/3} \\ &\quad + \frac{m_3^1(\theta_3)^2 \cdot X_b^2 \cdot X_b^3}{m_3^1(\theta_3) + X_b^2/2 + X_b^3/3} + \frac{m_3^1(\theta_3)^2 \cdot X_b^2 \cdot X_a^3}{m_3^1(\theta_3) + X_b^2/2 + X_a^3/2} \\ &= 0.1120 \\ m_{\text{PCR-CONVEX}}^1(\theta_4) &= \frac{m_4^1(\theta_4)^2 \cdot X_a^2 \cdot X_a^3}{m_4^1(\theta_4) + X_a^2/3 + X_a^3/2} + \frac{m_4^1(\theta_4)^2 \cdot X_a^2 \cdot X_b^3}{m_4^1(\theta_4) + X_a^2/3 + X_b^3/3} \\ &\quad + \frac{m_4^1(\theta_4)^2 \cdot X_b^2 \cdot X_b^3}{m_4^1(\theta_4) + X_b^2/2 + X_b^3/3} + \frac{m_4^1(\theta_4)^2 \cdot X_b^2 \cdot X_a^3}{m_4^1(\theta_4) + X_b^2/2 + X_a^3/2} \\ &= 0.1120 \end{aligned}$$

Table 4
The fusion results and Euclidean similarities of the methods.

	1	2	3	4
The fusion results by our method	0.0908, 0.1445, 0.1197, 0.4044, 0.2406	0.2229, 0.1445, 0.1327, 0.2250, 0.2749	0.2573, 0.2766, 0.1327, 0.2380, 0.0955	0.0778, 0.3109, 0.2648, 0.2380, 0.1085
The fusion results by PCR6 method	0.0909, 0.1451, 0.1194, 0.4045, 0.2401	0.2227, 0.1451, 0.1323, 0.2255, 0.2744	0.2570, 0.2768, 0.1323, 0.2384, 0.0954	0.0780, 0.3111, 0.2640, 0.2384, 0.1083
Euclidean similarities	99.94%	99.92%	99.95%	99.93%

$$\begin{aligned}
& m_{\text{PCR-CONVEX}}^1(\theta_5) \\
&= \frac{m_5^1(\theta_5)^2 \cdot X_a^2 \cdot X_a^3}{m_5^1(\theta_5) + X_a^2/3 + X_a^3/2} + \frac{m_5^1(\theta_5)^2 \cdot X_a^2 \cdot X_b^3}{m_5^1(\theta_5) + X_a^2/3 + X_b^3/3} \\
&+ \frac{m_5^1(\theta_5)^2 \cdot X_b^2 \cdot X_b^3}{m_5^1(\theta_5) + X_b^2/2 + X_b^3/3} + \frac{m_5^1(\theta_5)^2 \cdot X_b^2 \cdot X_a^3}{m_5^1(\theta_5) + X_b^2/2 + X_a^3/2} \\
&= 0.0572 \tag{55}
\end{aligned}$$

Similarly,

$$\begin{aligned}
m_{\text{PCR-CONVEX}}^2 &= [0.0572 \ 0.1118 \ 0.0047 \ 0.1118 \ 0.0348] \\
m_{\text{PCR-CONVEX}}^3 &= [0.0183 \ 0.0051 \ 0.1875 \ 0.1526 \ 0.0183] \tag{56}
\end{aligned}$$

Then the convex approximate result is obtained as follows

$$m_{\text{CONVEX}} = \{0.0923, 0.1337, 0.3042, 0.3764, 0.1103\} \tag{57}$$

3) The final approximate results are obtained by Equation (34)

$$m_{\text{GH}} = \{0.0908, 0.1315, 0.2991, 0.3701, 0.1085\} \tag{58}$$

4) The fusion results of DSMT + PCR6 are obtained as follows

$$m_{\text{DSMT+PCR6}} = \{0.0909, 0.1322, 0.2984, 0.3702, 0.1083\} \tag{59}$$

The Euclidean similarity between m_{GH} and m_{PCR6} is obtained by Equation (14)

$$E_{\text{GH}} = 99.93\% \tag{60}$$

From the above results of this example, the Euclidean similarity of the method in this paper can remain over 99.9% with DSMT + PCR6. It shows that the accuracy of the method in this paper is very high.

Example 2. Assume that there are the same 3 evidence sources as Example 1. $G_k^\ominus = \{\theta_1, \theta_2, \dots, \theta_5\}$, $k = 1, 2, 3$ denotes the hyper-power sets of the 3 evidence sources. The mass assignments in 3 evidences are $\mathbf{m}^1 = \{0.1, 0.1, 0.3, 0.3, 0.2\}$, $\mathbf{m}^2 = \{0.2, 0.3, 0.05, 0.3, 0.15\}$, $\mathbf{m}^3 = \{0.1, 0.05, 0.4, 0.35, 0.1\}$. Move the mass assignments of each focal element of \mathbf{m}^3 one position backward at one time and 4 new evidences are obtained by

$$\begin{aligned}
\mathbf{m}^3 &= \{0.1, 0.1, 0.05, 0.4, 0.35\}, \\
\mathbf{m}^3 &= \{0.35, 0.1, 0.1, 0.05, 0.4\} \\
\mathbf{m}^3 &= \{0.4, 0.35, 0.1, 0.1, 0.05\}, \\
\mathbf{m}^3 &= \{0.05, 0.4, 0.35, 0.1, 0.1\} \tag{61}
\end{aligned}$$

Each new evidence \mathbf{m}^3 and the original evidence \mathbf{m}^1 and \mathbf{m}^2 are combined to obtain the fusion results by DSMT + PCR6 and the method in this paper. Then Euclidean similarities of two fusion results are obtained by Equation (14). The fusion results and Euclidean similarities of two methods are shown as Table 4.

As shown in Table 1, the Euclidean similarities of the method in this paper with DSMT + PCR6 all remain over 99.9% and change little. It shows that the method in this paper has not only very high accuracy, but also high performance stability.

4.2. Complex cases of both singleton focal elements and multiple focal elements in evidences

Example 3. Assume that there are 3 evidence sources and the hyper-power sets are denoted by $G_k^\ominus = \{\theta_1 \cup \theta_2, \theta_1, \theta_2, \theta_3, \theta_4, \theta_5, \theta_6, \theta_7\}$, $k = 1, 2, 3$. The mass assignments of evidences are denoted by $\mathbf{m}^1 = \{0.2, 0.1, 0.1, 0.1, 0.3, 0.1, 0.05, 0.05\}$, $\mathbf{m}^2 = \{0.05, 0.2, 0.3, 0.05, 0.25, 0.01, 0.1, 0.04\}$, $\mathbf{m}^3 = \{0.1, 0.1, 0.04, 0.4, 0.15, 0.1, 0.1, 0.01\}$, the method process in this paper is given as follows

1) The mass assignments of focal elements in each evidence is clustered to two sets by the Evidence Clustering method as follows

$$\begin{aligned}
x_a^1 &= \{\theta_1 \cup \theta_2, \theta_4\}, & x_b^1 &= \{\theta_1, \theta_2, \theta_3, \theta_5, \theta_6, \theta_7\} \\
x_a^2 &= \{\theta_1 \cup \theta_2, \theta_1, \theta_2, \theta_3, \theta_4, \theta_6, \theta_7\}, & x_b^2 &= \{\theta_5\} \\
x_a^3 &= \{\theta_3, \theta_4\}, & x_b^3 &= \{\theta_1 \cup \theta_2, \theta_1, \theta_2, \theta_5, \theta_6, \theta_7\} \tag{62}
\end{aligned}$$

Then

$$\begin{aligned}
X_a^1 &= 0.5, & X_b^1 &= 0.5; & X_a^2 &= 0.99; & X_b^2 &= 0.01; \\
X_a^3 &= 0.55; & X_b^3 &= 0.45 \tag{63}
\end{aligned}$$

2) The convex function approximate fusion results are calculated by Equation (32)

$$\begin{aligned}
m_{\text{PCR-CONVEX}}^1 &= \{0.0792, 0.0250, 0.0250, 0.0250, 0.1479, \\
& \quad 0.0250, 0.0072, 0.0072\} \\
m_{\text{PCR-CONVEX}}^2 &= \{0.0071, 0.0771, 0.1442, 0.0071, 0.1093, \\
& \quad 0.0003, 0.0244, 0.0047\} \\
m_{\text{PCR-CONVEX}}^3 &= \{0.0257, 0.0257, 0.0049, 0.2297, 0.0510, \\
& \quad 0.0257, 0.0257, 0.0003\} \tag{64}
\end{aligned}$$

3) Then the normalized approximate convex results are obtained as follows

$$\begin{aligned}
m_{\text{CONVEX}} &= \{0.1014, 0.1157, 0.1576, 0.2370, 0.2791, \\
& \quad 0.0462, 0.0519, 0.0111\} \tag{65}
\end{aligned}$$

4) For the singleton focal elements $\theta_3, \theta_4, \theta_5, \theta_6, \theta_7$ which are not involved in the multiple focal elements, the approximate convex results of these focal elements are unchanged. For the multiple focal element $\theta_1 \cup \theta_2$ and the singleton focal elements θ_1 and θ_2 , the convex approximate fusion results should be changed as follows

$m_{\text{PCR-CONVEX}}^1(\theta_1 \cup \theta_2)$ has the wrong proportional mass assignments from the following items

$$\begin{aligned}
& m^1(\theta_1 \cup \theta_2) \otimes m^2(\theta_1) \otimes m^3(\theta_1), m^1(\theta_1 \cup \theta_2) \otimes m^2(\theta_2) \otimes m^3(\theta_2), \\
& m^1(\theta_1 \cup \theta_2) \otimes m^2(\theta_1 \cup \theta_2) \otimes m^3(\theta_1), m^1(\theta_1 \cup \theta_2) \otimes m^2(\theta_1) \\
& \quad \otimes m^3(\theta_1 \cup \theta_2), \\
& m^1(\theta_1 \cup \theta_2) \otimes m^2(\theta_1 \cup \theta_2) \otimes m^3(\theta_2), m^1(\theta_1 \cup \theta_2) \otimes m^2(\theta_2) \\
& \quad \otimes m^3(\theta_1 \cup \theta_2)
\end{aligned}$$

which should be the mass assignments of $m_{\text{PCR-CONVEX}}^1(\theta_1)$ and $m_{\text{PCR-CONVEX}}^1(\theta_2)$. Similarly, $m_{\text{PCR-CONVEX}}^2(\theta_1 \cup \theta_2)$, $m_{\text{PCR-CONVEX}}^3(\theta_1 \cup \theta_2)$ also have the wrong proportional mass assignment. So, the

Table 5

Euclidean similarities of the results of the method in this paper with DSMT + PCR6.

Experiment times	1	2	3	4	5	6	7
Euclidean similarities	99.49%	99.46%	99.42%	99.41%	99.38%	99.46%	99.29%

proportional mass assignments of θ_1 or θ_2 generated by $\theta_1 \cup \theta_2$ are calculated as follows

$$\begin{aligned} m\text{-multiple}^1(\theta_1, \theta_2) &= \{0.0038, 0.0032\} \\ m\text{-multiple}^2(\theta_1, \theta_2) &= \{0.0003, 0.0003\} \\ m\text{-multiple}^3(\theta_1, \theta_2) &= \{0.0015, 0.0018\} \end{aligned} \quad (66)$$

Then

$$\begin{aligned} m_{GH}(\theta_1 \cup \theta_2) &= m_{CONVEX}(\theta_1 \cup \theta_2) - \sum_{j=1,2,3} m\text{-multiple}^j(\theta_1) \\ &\quad - \sum_{j=1,2,3} m\text{-multiple}^j(\theta_2) \end{aligned} \quad (67)$$

$$m_{GH}(\theta_1) = m_{CONVEX}(\theta_1) + \sum_{j=1,2,3} m\text{-multiple}^j(\theta_1) \quad (68)$$

$$m_{GH}(\theta_2) = m_{CONVEX}(\theta_2) + \sum_{j=1,2,3} m\text{-multiple}^j(\theta_2) \quad (69)$$

The final approximate results are obtained as follows

$$m_{GH} = \{0.0906, 0.1214, 0.1628, 0.2370, 0.2791, 0.0462, 0.0519, 0.0111\} \quad (70)$$

4) The fusion results of DSMT + PCR6 are obtained as follows

$$m_{DSMT+PCR6} = \{0.0858, 0.1232, 0.1678, 0.2380, 0.2789, 0.0441, 0.0515, 0.0107\} \quad (71)$$

The Euclidean similarity between m_{GH} and m_{PCR6} is obtained by Equation (14)

$$E_{GH} = 99.46\% \quad (72)$$

It can be drawn in the above experiment results that in the complex cases of both singleton focal elements and multiple focal elements in evidences, the Euclidean similarities of the method in this paper with DSMT + PCR6 also remain over 99%. It shows that the method in this paper is also fit for the complex cases.

Example 4. Assume that there are the same evidence sources as Example 3 and $G_k^\ominus = \{\theta_1 \cup \theta_2, \theta_1, \theta_2, \theta_3, \theta_4, \theta_5, \theta_6, \theta_7\}$, $k = 1, 2, 3$ denotes the hyper-power sets. Move the mass assignments of \mathbf{m}^3 one position backward at one time to procedure 7 new evidences.

The new 3 evidences are combined by DSMT + PCR6 and the method in this paper. Then Euclidean similarities of two fusion results are obtained by Equation (9). Euclidean similarities of two methods are shown as Table 5.

As shown in Table 2, in the complex cases of both singleton focal elements and multiple focal elements in evidences, the method in this paper has not only very high accuracy which remains the Euclidean similarities with DSMT + PCR6 over 99%, but also very high performance stability.

4.3. Associative analysis

Example 5. Assume that there are 3 evidence sources and the hyper-power sets are denoted by $G_k^\ominus = \{\theta_1, \theta_2, \dots, \theta_5\}$, $k = 1, 2, 3$. The mass assignments in each evidence are the same as Example 1 which are $\mathbf{m}^1 = \{0.1, 0.1, 0.3, 0.3, 0.2\}$, $\mathbf{m}^2 = \{0.2, 0.3, 0.05, 0.3, 0.15\}$, $\mathbf{m}^3 = \{0.1, 0.05, 0.4, 0.35, 0.1\}$.

1) The fusion sequence $\mathbf{m}^1 \rightarrow \mathbf{m}^2 \rightarrow \mathbf{m}^3$ is applied. The fusion results are from Example 1 as follows

$$m_{GH} = \{0.0908, 0.1315, 0.2991, 0.3701, 0.1085\}$$

2) The fusion sequence $\mathbf{m}^1 \rightarrow \mathbf{m}^3 \rightarrow \mathbf{m}^2$ is applied. The fusion process is given by

(1) The mass assignments of focal elements in each evidence are clustered to two sets by the Evidence Clustering method, denoted by

$$\begin{aligned} x_a^1 &= \{\theta_3, \theta_4, \theta_5\}, & x_b^1 &= \{\theta_1, \theta_2\}; \\ x_a^3 &= \{\theta_4, \theta_5\}, & x_b^3 &= \{\theta_1, \theta_2, \theta_3\}; \\ x_a^2 &= \{\theta_1, \theta_2, \theta_4, \theta_5\}, & x_b^2 &= \{\theta_3\} \end{aligned} \quad (73)$$

Then

$$\begin{aligned} X_a^1 &= 0.8, & X_b^1 &= 0.2; & X_a^3 &= 0.75, & X_b^3 &= 0.25; \\ X_a^2 &= 0.95, & X_b^2 &= 0.05 \end{aligned} \quad (74)$$

(2) The convex function approximate fusion results are calculated by Equation (32)

$$\begin{aligned} m\text{-convex}_1^1(\theta_1) &= \frac{m_1^1(\theta_1)^2 \cdot X_a^3 \cdot X_a^2}{m_1^1(\theta_1) + X_a^3/2 + X_a^2/3} + \frac{m_1^1(\theta_1)^2 \cdot X_b^3 \cdot X_b^2}{m_1^1(\theta_1) + X_b^3/3 + X_b^2/3} \\ &\quad + \frac{m_1^1(\theta_1)^2 \cdot X_b^3 \cdot X_b^2}{m_1^1(\theta_1) + X_b^3/3 + X_b^2/2} + \frac{m_1^1(\theta_1)^2 \cdot X_a^3 \cdot X_b^2}{m_1^1(\theta_1) + X_a^3/2 + X_b^2/2} \\ &= 0.0169 \end{aligned}$$

$$\begin{aligned} m\text{-convex}_2^1(\theta_2) &= \frac{m_2^1(\theta_2)^2 \cdot X_a^3 \cdot X_a^2}{m_2^1(\theta_2) + X_a^3/2 + X_a^2/3} + \frac{m_2^1(\theta_2)^2 \cdot X_b^3 \cdot X_b^2}{m_2^1(\theta_2) + X_b^3/3 + X_b^2/3} \\ &\quad + \frac{m_2^1(\theta_2)^2 \cdot X_b^3 \cdot X_b^2}{m_2^1(\theta_2) + X_b^3/3 + X_b^2/2} + \frac{m_2^1(\theta_2)^2 \cdot X_a^3 \cdot X_b^2}{m_2^1(\theta_2) + X_a^3/2 + X_b^2/2} \\ &= 0.0169 \end{aligned}$$

$$\begin{aligned} m\text{-convex}_3^1(\theta_3) &= \frac{m_3^1(\theta_3)^2 \cdot X_a^3 \cdot X_a^2}{m_3^1(\theta_3) + X_a^3/2 + X_a^2/3} + \frac{m_3^1(\theta_3)^2 \cdot X_b^3 \cdot X_b^2}{m_3^1(\theta_3) + X_b^3/3 + X_b^2/3} \\ &\quad + \frac{m_3^1(\theta_3)^2 \cdot X_b^3 \cdot X_b^2}{m_3^1(\theta_3) + X_b^3/3 + X_b^2/2} + \frac{m_3^1(\theta_3)^2 \cdot X_a^3 \cdot X_b^2}{m_3^1(\theta_3) + X_a^3/2 + X_b^2/2} \\ &= 0.1120 \end{aligned}$$

$$\begin{aligned} m\text{-convex}_4^1(\theta_4) &= \frac{m_4^1(\theta_4)^2 \cdot X_a^3 \cdot X_a^2}{m_4^1(\theta_4) + X_a^3/2 + X_a^2/3} + \frac{m_4^1(\theta_4)^2 \cdot X_b^3 \cdot X_b^2}{m_4^1(\theta_4) + X_b^3/3 + X_b^2/3} \\ &\quad + \frac{m_4^1(\theta_4)^2 \cdot X_b^3 \cdot X_b^2}{m_4^1(\theta_4) + X_b^3/3 + X_b^2/2} + \frac{m_4^1(\theta_4)^2 \cdot X_a^3 \cdot X_b^2}{m_4^1(\theta_4) + X_a^3/2 + X_b^2/2} \\ &= 0.1120 \end{aligned}$$

$$\begin{aligned} m\text{-convex}_5^1(\theta_5) &= \frac{m_5^1(\theta_5)^2 \cdot X_a^3 \cdot X_a^2}{m_5^1(\theta_5) + X_a^3/2 + X_a^2/3} + \frac{m_5^1(\theta_5)^2 \cdot X_b^3 \cdot X_b^2}{m_5^1(\theta_5) + X_b^3/3 + X_b^2/3} \end{aligned}$$

Table 6
The mass assignments of the focal elements of four evidence sources.

Highly conflict sources	θ_1	θ_2	θ_3	θ_4
S_1	$x - 0.01$	0.01	$1 - x - 0.01$	0.01
S_2	0.01	$y - 0.01$	0.01	$1 - y - 0.01$
S_3	0.01	$x - 0.01$	$1 - x - 0.01$	0.01
S_4	$y - 0.01$	$1 - y - 0.01$	0.01	0.01

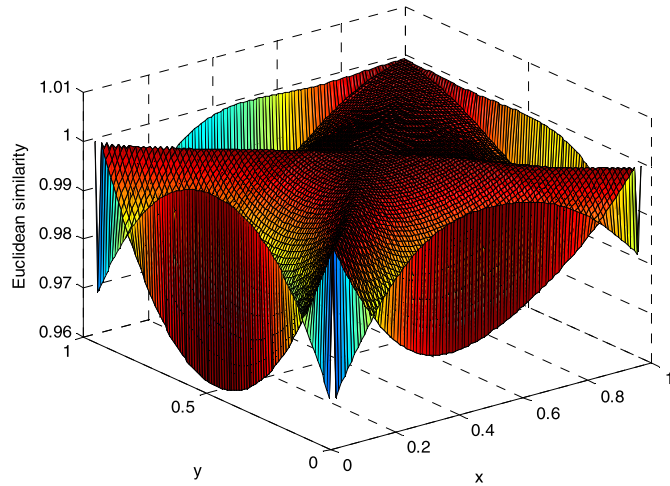


Fig. 1. Euclidean similarities of the method in this paper with DSMT + PCR6.

$$\begin{aligned}
 & + \frac{m_5^1(\theta_5)^2 \cdot X_b^3 \cdot X_b^2}{m_5^1(\theta_5) + X_b^3/3 + X_b^2/2} + \frac{m_5^1(\theta_5)^2 \cdot X_a^3 \cdot X_b^2}{m_5^1(\theta_5) + X_a^3/2 + X_b^2/2} \\
 & = 0.0572
 \end{aligned} \quad (75)$$

Similarly,

$$\begin{aligned}
 m\text{-convex}^2 &= [0.0572 \ 0.1118 \ 0.0047 \ 0.1118 \ 0.0348] \\
 m\text{-convex}^3 &= [0.0183 \ 0.0051 \ 0.1875 \ 0.1526 \ 0.0183]
 \end{aligned} \quad (76)$$

Then the convex approximate result is obtained as follows

$$m_{\text{CONVEX}} = \{0.0923, 0.1337, 0.3042, 0.3764, 0.1103\} \quad (77)$$

3) The final approximate results are obtained by Equation (34)

$$m_{\text{GH}} = \{0.0908, 0.1315, 0.2991, 0.3701, 0.1085\} \quad (78)$$

By comparing the fusion process with Example 1, it can be drawn that the method in this paper has the associative property as the convex function approximate results of Equation (32) are unchanged with different fusion sequences.

4.4. Cases of highly conflict evidence sources

Example 6. Assume that there are four highly conflict evidence sources, and the hyper-power set of the four evidence sources are denoted by $D^\ominus = \{\theta_1, \theta_2, \theta_3, \theta_4\}$. The mass assignments of the focal elements of four evidence sources are shown as Table 6.

Let $x, y \in [0.02, 0.98]$ and x, y increases from 0.02 to 0.98 by 0.01 step. With the different values of x, y , Euclidean similarities of the method in this paper with DSMT + PCR6 are shown as Fig. 1. The average Euclidean similarity is also calculated as 99.17%.

From Fig. 1 and the average Euclidean similarity, it can be drawn that under Cases of highly conflict evidence sources, the method in this paper can also get very high similar fusion results with DSMT + PCR6 which remains Euclidean similarities over 99% in the experiments and solve the highly conflict evidences fusion problems effectively.

4.5. Convergence analysis

Example 7. Assume that there are 4 evidence sources and the hyper-power sets of the evidence sources are denoted by $G_k^\ominus = \{\theta_1, \theta_2, \dots, \theta_6\}$, $k = 1, 2, 3, 4$. The mass assignments in evidences are $\mathbf{m}^1 = \{0.01, 0.11, 0.35, 0.23, 0.15, 0.15\}$, $\mathbf{m}^2 = \{0.01, 0.11, 0.23, 0.35, 0.15, 0.15\}$, $\mathbf{m}^3 = \{0.5, 0.3, 0.05, 0.05, 0.05, 0.05\}$, $\mathbf{m}^4 = \{0.4, 0.2, 0.1, 0.1, 0.1, 0.1\}$. Three methods are applied in this experiment to compare the convergence speeds. The methods are DSMT + PCR6, the method in this paper and the DST combination method.

First, fusion results of four evidences are obtained by different fusion methods. Then, the prior fusion results of the last time are fused with $\mathbf{m}^3, \mathbf{m}^4$ repeatedly. The fusion results by different methods for convergence analysis are calculated as Table 7.

It can be drawn from Table 7 that

1) The convergence speed of the method in this paper is faster than DSMT + PCR6 which converge to $\{0.7617, 0.1749, 0.0158, 0.0158, 0.0158, 0.0158\}$ in the 14th experiment and DSMT + PCR6 converge to $\{0.7749, 0.1650, 0.0150, 0.0150, 0.0150, 0.0150\}$ in the 18th experiment.

2) The convergence speed of the DST combination method is the fastest one among the three methods which converge to $\{1.0000, 0.0000, 0.0000, 0.0000, 0.0000, 0.0000\}$ in the 12th experiment, but this fusion result is strong converge to θ_1 and it is unchanged and wrong even if the following evidences focus on the other elements. Besides, the first two experiments' results of DST are not reasonable for the high conflict evidences in these experiments.

From the above convergence analysis, it shows that the method in this paper has good convergence speed and the convergence results are also reasonable and effective.

4.6. Monte Carlo simulation experiments in the case of random mass assignments in evidences

Example 8. Assume that there are three evidence sources. The hyper-power sets of the sources are denoted by $P^\ominus = \{\theta_1, \theta_2, \dots, \theta_{20}\}$ and only singleton focal elements have mass assignments. Monte Carlo simulation experiments are carried out 1000 times. The mass assignments of 20 focal elements in evidences are assigned randomly each time. The fusion results of three random evidences are obtained by DSMT + PCR6 and the method in this paper. Then the Euclidean similarities of the method in this paper with DSMT + PCR6 are calculated and the computing time of methods are recorded as shown in Fig. 2, Fig. 3 and Table 8. (In this paper, all the simulation experiments are implemented by Matlab simulation in the hardware condition of Pentium^(R) Dual-Core CPU E5300 2.6 GHz 2.59 GHz, memory 1.99 GB.)

It can be drawn from Fig. 3, Fig. 4 and Table 8 that, in the case of random mass assignments in evidences, the method in this paper remains high Euclidean similarity and the average Euclidean similarity can reach 99.81%. Moreover, Euclidean similarity changes very little when the evidences are changed. Computing time of the method in this paper is much smaller than DSMT + PCR6. The simulation experiments results show that the method in this paper has strong practical meaning.

4.7. Monte Carlo simulations in the case of increasing focal elements number and sources number

Example 9. In this section, Monte Carlo simulation experiments in the case of increasing focal elements number and sources number are performed. Assume that only singleton focal elements have mass assignments in hyper-power sets and the mass assignments

Table 7
Fusion results by different methods for convergence analysis.

Experiment times	DSmT + PCR6	The method in this paper Fusion results	DST
1	0.5811, 0.2209, 0.0688, 0.0688, 0.0302, 0.0302	0.5796, 0.2218, 0.0681, 0.0681, 0.0312, 0.0312	0.0759, 0.8264, 0.0382, 0.0382, 0.0170, 0.0170
2	0.6845, 0.2200, 0.0272, 0.0272, 0.0205, 0.0205	0.6824, 0.2217, 0.0272, 0.0272, 0.0208, 0.0208	0.2326, 0.7599, 0.0029, 0.0029, 0.0008, 0.0008
3	0.7284, 0.2022, 0.0177, 0.0177, 0.0171, 0.0171	0.7245, 0.2049, 0.0179, 0.0179, 0.0174, 0.0174	0.5048, 0.4948, 0.0002, 0.0002, 0.0000, 0.0000
4	0.7494, 0.1870, 0.0159, 0.0159, 0.0159, 0.0159	0.7433, 0.1913, 0.0164, 0.0164, 0.0163, 0.0163	0.7728, 0.2272, 0.0000, 0.0000, 0.0000, 0.0000
5	0.7607, 0.1775, 0.0154, 0.0154, 0.0154, 0.0154	0.7525, 0.1834, 0.0160, 0.0160, 0.0160, 0.0160	0.9189, 0.0811, 0.0000, 0.0000, 0.0000, 0.0000
6	0.7670, 0.1719, 0.0153, 0.0153, 0.0153, 0.0153	0.7571, 0.1792, 0.0159, 0.0159, 0.0159, 0.0159	0.9742, 0.0258, 0.0000, 0.0000, 0.0000, 0.0000
7	0.7705, 0.1688, 0.0152, 0.0152, 0.0152, 0.0152	0.7594, 0.1770, 0.0159, 0.0159, 0.0159, 0.0159	0.9921, 0.0079, 0.0000, 0.0000, 0.0000, 0.0000
8	0.7725, 0.1671, 0.0151, 0.0151, 0.0151, 0.0151	0.7605, 0.1760, 0.0159, 0.0159, 0.0159, 0.0159	0.9976, 0.0024, 0.0000, 0.0000, 0.0000, 0.0000
9	0.7735, 0.1662, 0.0151, 0.0151, 0.0151, 0.0151	0.7611, 0.1755, 0.0159, 0.0159, 0.0159, 0.0159	0.9993, 0.0007, 0.0000, 0.0000, 0.0000, 0.0000
10	0.7741, 0.1656, 0.0151, 0.0151, 0.0151, 0.0151	0.7614, 0.1752, 0.0159, 0.0159, 0.0159, 0.0159	0.9998, 0.0002, 0.0000, 0.0000, 0.0000, 0.0000
11	0.7745, 0.1653, 0.0151, 0.0151, 0.0151, 0.0151	0.7615, 0.1751, 0.0159, 0.0159, 0.0159, 0.0159	0.9999, 0.0001, 0.0000, 0.0000, 0.0000, 0.0000
12	0.7746, 0.1652, 0.0150, 0.0150, 0.0150, 0.0150	0.7616, 0.1750, 0.0158, 0.0158, 0.0158, 0.0158	1.0000, 0.0000, 0.0000, 0.0000, 0.0000, 0.0000
13	0.7747, 0.1651, 0.0150, 0.0150, 0.0150, 0.0150	0.7616, 0.1750, 0.0158, 0.0158, 0.0158, 0.0158	1.0000, 0.0000, 0.0000, 0.0000, 0.0000, 0.0000
14	0.7748, 0.1650, 0.0150, 0.0150, 0.0150, 0.0150	0.7617, 0.1750, 0.0158, 0.0158, 0.0158, 0.0158	1.0000, 0.0000, 0.0000, 0.0000, 0.0000, 0.0000
15	0.7748, 0.1650, 0.0150, 0.0150, 0.0150, 0.0150	0.7617, 0.1749, 0.0158, 0.0158, 0.0158, 0.0158	1.0000, 0.0000, 0.0000, 0.0000, 0.0000, 0.0000
16	0.7748, 0.1650, 0.0150, 0.0150, 0.0150, 0.0150	0.7617, 0.1749, 0.0158, 0.0158, 0.0158, 0.0158	1.0000, 0.0000, 0.0000, 0.0000, 0.0000, 0.0000
17	0.7748, 0.1650, 0.0150, 0.0150, 0.0150, 0.0150	0.7617, 0.1749, 0.0158, 0.0158, 0.0158, 0.0158	1.0000, 0.0000, 0.0000, 0.0000, 0.0000, 0.0000
18	0.7749, 0.1650, 0.0150, 0.0150, 0.0150, 0.0150	0.7617, 0.1749, 0.0158, 0.0158, 0.0158, 0.0158	1.0000, 0.0000, 0.0000, 0.0000, 0.0000, 0.0000
19	0.7749, 0.1650, 0.0150, 0.0150, 0.0150, 0.0150	0.7617, 0.1749, 0.0158, 0.0158, 0.0158, 0.0158	1.0000, 0.0000, 0.0000, 0.0000, 0.0000, 0.0000
20	0.7749, 0.1650, 0.0150, 0.0150, 0.0150, 0.0150	0.7617, 0.1749, 0.0158, 0.0158, 0.0158, 0.0158	1.0000, 0.0000, 0.0000, 0.0000, 0.0000, 0.0000

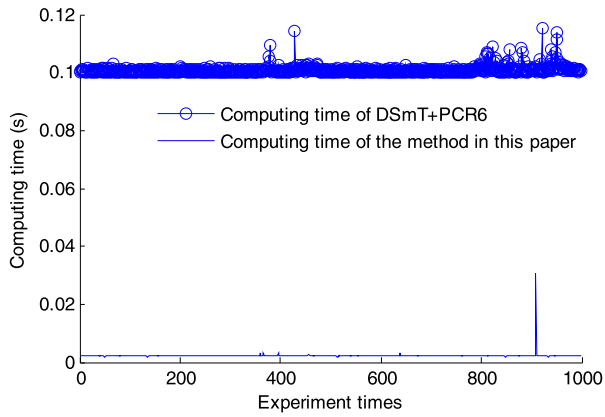


Fig. 2. Computing time of the method in this paper and DSMT + PCR6.

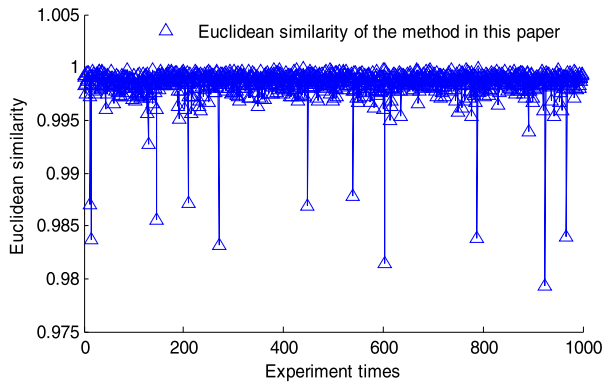


Fig. 3. Euclidean similarity of the method in this paper with DSMT + PCR6.

of the focal elements are assigned randomly each time. The experiments consist of four cases. In the cases 1–3, the number of focal elements increases with the constant number of evidence sources.

Table 8
Fusion results comparison in the case of random mass assignments.

	Average Euclidean similarity	Max Euclidean similarity	Min Euclidean similarity	Average computing time (s)	Max computing time (s)	Min computing time (s)
DSmT + PCR5				0.1008	0.1153	0.1000
The method in this paper	99.81%	99.98%	97.92%	0.0021	0.0306	0.0019

It can be drawn from the Table 3 that the computation complexity of PCR6 method is too large to make simulations when the number of sources is big. So the maximum number of evidence sources in cases 1–3 is set to be 5 and the number of focal elements is no more than 20 in the third case. In the fourth case, the number of evidence sources increases with the constant number of focal elements. Also for the large computation complexity of PCR6, the maximum number of sources is considered as 10, and each evidence is composed of 5 focal elements.

The simulation experiments are given as follows

1) Assume that there are 3 evidence sources, and the focal elements of the hyper-power sets increase one focal element from 10 to 100. The Euclidean similarities and computing time with the increment of the number of focal elements is recorded as shown in Figs. 4–5.

2) Assume that there are 4 evidence sources, and the focal elements of the hyper-power sets increase one focal element from 10 to 50. The Euclidean similarities and computing time with the increment of the number of focal elements is recorded as shown in Figs. 6–7.

3) Assume that there are 5 evidence sources, and the focal elements of the hyper-power sets increase one focal element from 10 to 20. For The Euclidean similarities and computing time with the increment of the number of focal elements is recorded as shown in Figs. 8–9.

4) Assume that there are 5 focal elements, and the number of evidence sources increases one by one from 3 to 10. The Euclidean similarities and computing time with the increment of the number of sources is shown in Figs. 10–11. Especially, in order to explicitly present the increment of computing time, the ordinate scale is log instead of linear in Fig. 11.

As shown in Figs. 4–11,

1) The computing time of DSMT + PCR6 increases exponentially with the linear increment of the number of the focal elements. However, the computing time of the method in this paper increases almost linearly with the linear increment of the

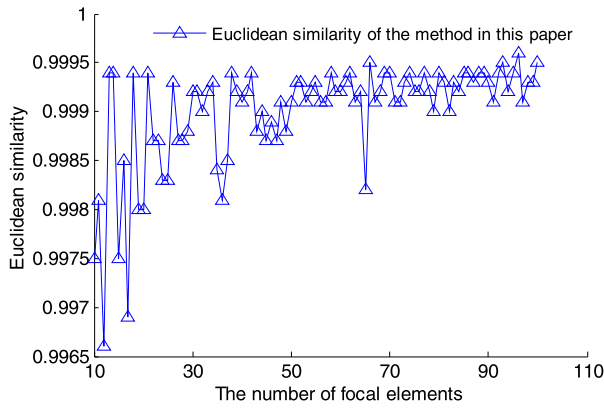


Fig. 4. Euclidean similarity of the method in this paper with DSMT + PCR6.

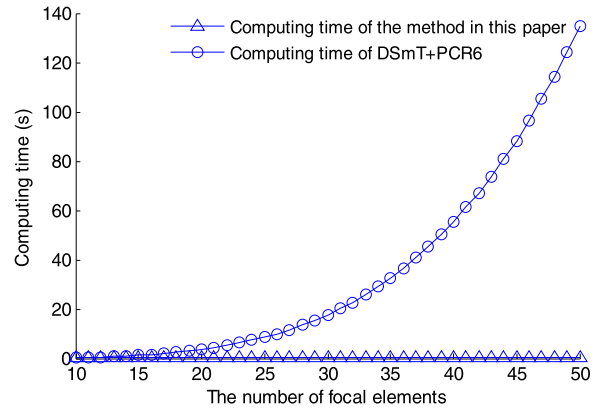


Fig. 7. Computing time of the method in this paper and DSMT + PCR6.

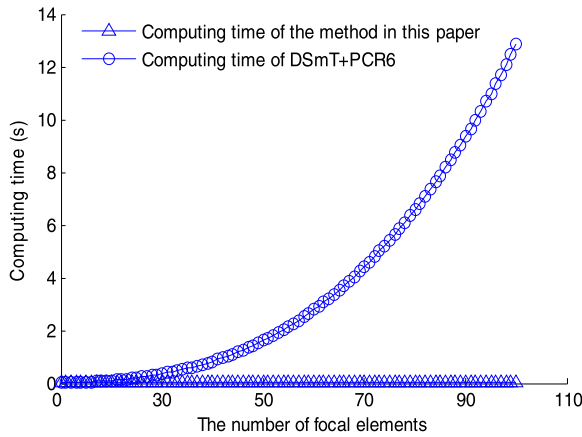


Fig. 5. Computing time of the method in this paper and DSMT + PCR6.

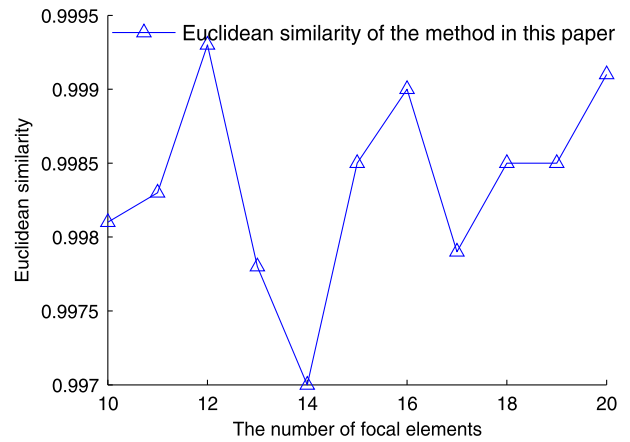


Fig. 8. Euclidean similarity of the method in this paper with DSMT + PCR6.

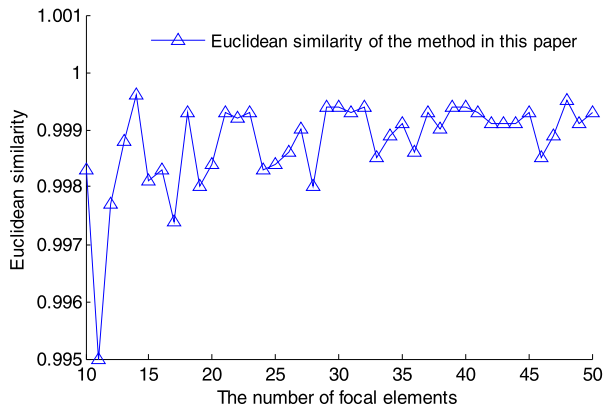


Fig. 6. Euclidean similarity of the method in this paper with DSMT + PCR6.

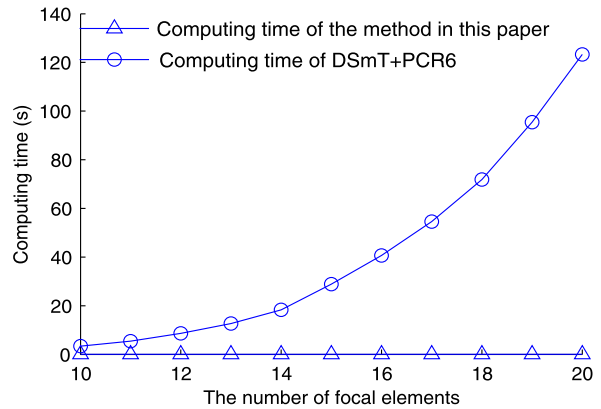


Fig. 9. Computing time of the method in this paper and DSMT + PCR6.

number of the focal elements and remains very low computation time.

2) The computing time of DSMT + PCR6 increases huge rapidly when the sources number increases. When there are 5 sources and 20 focal elements, the computing time of DSMT + PCR6 is 123.2790 seconds. Whereas, in the case of 10 sources and 5 focal elements, its computing time reaches 1213.9 seconds. It shows that when the number of evidence sources is large, DSMT + PCR6 takes too big computation burden, and it is hard to satisfy the real-time requirement of intelligent systems. However, the computing time of the method in this paper increases little with the increment of evidence sources and it remains very little computing time which can satisfy the real-time requirements of intelligent systems.

3) In different conditions, the Euclidean similarities of the method in this paper with DSMT + PCR6 all remain over 99% and converge to very high value with the increment of the number of the focal elements. It shows that the method in this paper can obtain very similar approximate fusion results with DSMT + PCR6, especially when the number of focal elements is large.

5. Conclusions

To get high similar approximate reasoning results with DSMT + PCR6 and remain less computation complexity, an Evidence Clustering DSMT approximate reasoning method for more than two

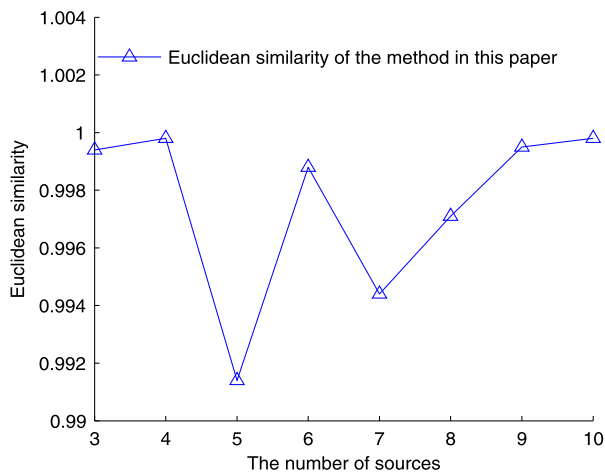


Fig. 10. Euclidean similarity of the method in this paper with DSMT + PCR6.

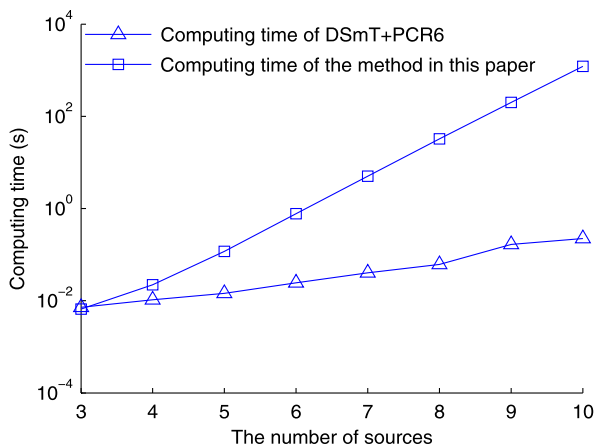


Fig. 11. Computing time of the method in this paper and DSMT + PCR6.

sources is proposed in this paper. Firstly, the focal elements of multi evidences are clustered to two sets by their mass assignments respectively. Secondly, the convex approximate fusion results are obtained by the new DSMT approximate formula for more than two sources. Thirdly, the final approximate fusion results by the method in this paper are obtained by the normalization step. Analysis of computation complexity show that the method in this paper cost much less computation complexity than DSMT + PCR6. The simulation experiments show that the method in this paper can get very similar approximate fusion results and need much less computing time than DSMT + PCR6, especially, when the numbers of sources and focal elements are large, the superiorities of the method are remarkable.

However, the mathematical analysis of convergence of the proposed method and the other evidence reasoning methods are still important tasks in our future research plans. We will also apply this new method in some real practical areas like radar signal combinations in our future work.

Acknowledgments

The authors extremely appreciate Editor-in-chief Ercan Engin Kuruoglu for his encouragement and appreciation to our research. We are also grateful to Prof. F. Smarandache, Prof. De-cun Zhang, Prof. Xinde Li and Prof. Zhunga Liu for discussions. We are also very grateful to all the anonymous reviewers for their critical and constructive review of the manuscript. This study was co-supported by the National Natural Science Foundation of China

(Nos. 61102166 and 61471379) and Science and Technology Major Project of Shandong Province (No. 2015ZDZX01001).

Appendix A. Supplementary material

Supplementary material related to this article can be found online at <http://dx.doi.org/10.1016/j.dsp.2016.05.007>.

References

- [1] Ashirbani Saha, Gaurav Bhatnagar, Q.M. Jonathan Wu, Mutual spectral residual approach for multifocus image fusion, *Digit. Signal Process.* 23 (4) (2013) 1121–1135.
- [2] Ammar Cherchar, Messaoud Thameri, Adel Belouchrani, Performance improvement of direction finding algorithms in non-homogeneous environment through data fusion, *Digit. Signal Process.* 41 (2015) 41–47.
- [3] Alan J. Terry, Munir Zaman, John Illingworth, Sensor fusion by a novel algorithm for time delay estimation, *Digit. Signal Process.* 22 (3) (2012) 439–452.
- [4] Hong Jiang, Kun Zhan, Long Xu, Joint tracking and classification with constraints and reassignment by radar and ESM, *Digit. Signal Process.* 40 (2015) 213–223.
- [5] Yi Yang, Deqiang Han, Chongzhao Han, Discounted combination of unreliable evidence using degree of disagreement, *Int. J. Approx. Reason.* 54 (8) (2013) 1197–1216.
- [6] Tao Jian, You He, Feng Su, Xiaodong Huang, Dianfa Ping, Adaptive detection of range-spread targets without secondary data in multichannel autoregressive process, *Digit. Signal Process.* 23 (5) (2013) 1684–1694.
- [7] You He, Cai-sheng Zhang, Xiao-ming Tang, Xiao-jun Chu, Jia-hui Ding, Coherent integration loss due to pulses loss and phase modulation in passive bistatic radar, *Digit. Signal Process.* 23 (4) (2013) 1265–1276.
- [8] X. Li, J. Dezert, F. Smarandache, X. Dai, Combination of qualitative information based on 2-tuple modelings in DSMT, *J. Comput. Sci. Technol.* 24 (4) (2009) 786–798.
- [9] X. Li, J. Dezert, F. Smarandache, Fusion of imprecise qualitative information, *Appl. Intell.* 33 (3) (2010) 340–351.
- [10] T. Denoeux, N. El Zoghby, V. Cherfaoui, A. Jouglet, Optimal object association in the Dempster–Shafer framework, *IEEE Trans. Cybern.* 44 (22) (2014) 2521–2531.
- [11] Qiang Guo, You He, Xin Guan, et al., An evidence clustering DSMT approximate reasoning method based on convex functions analysis, *Digit. Signal Process.* 45 (2015) 13–23.
- [12] F. Smarandache, J. Dezert, *Advances and Applications of DSMT for Information Fusion*, vols. 1–4, American Research Press, Rehoboth, USA, 2004/2006/2009/2015.
- [13] G. Shafer, *A Mathematical Theory of Evidence*, Princeton Univ. Press, Princeton, NJ, 1976.
- [14] G. Shafer, Perspectives on the theory and practice of belief functions, *Int. J. Approx. Reason.* 4 (1990) 323–362.
- [15] R. Singh, M. Vatsa, A. Noore, Integrated multilevel image fusion and match score fusion of visible and infrared face images for robust face recognition, *Pattern Recognit.* 41 (3) (2008) 880–893.
- [16] Z. Liu, J. Dezert, Q. Pan, G. Mercier, Combination of sources of evidence with different discounting factors based on a new dissimilarity measure, *Decis. Support Syst.* 52 (1) (2011) 133–141.
- [17] S. Huang, X. Su, Y. Hu, S. Mahadevan, Y. Deng, A new decision-making method by incomplete preferences based on evidence distance, *Knowl.-Based Syst.* 56 (2014) 264–272.
- [18] F. Faux, F. Luthon, Theory of evidence for face detection and tracking, *Int. J. Approx. Reason.* 53 (5) (2012) 728–746.
- [19] Z. Liu, J. Dezert, G. Mercier, Q. Pan, Dynamic evidential reasoning for change detection in remote sensing images, *IEEE Trans. Geosci. Remote Sens.* 50 (5) (2012) 1955–1967.
- [20] X. Li, X. Huang, J. Dezert, et al., A successful application of DSMT in sonar grid map building and comparison with DST-based approach, *Int. J. Innov. Comput. Inf. Control* 3 (3) (2007) 539–551.
- [21] Z. Liu, Q. Pan, J. Dezert, Evidential classifier for imprecise data based on belief functions, *Knowl.-Based Syst.* 52 (2013) 246–257.
- [22] Z. Liu, Q. Pan, J. Dezert, G. Mercier, Credal classification rule for uncertain data based on belief functions, *Pattern Recognit.* 47 (7) (2014) 2532–2541.
- [23] Z. Liu, Q. Pan, G. Mercier, J. Dezert, A new incomplete pattern classification method based on evidential reasoning, *IEEE Trans. Cybern.* 45 (4) (2015) 635–646.
- [24] C. Lian, S. Ruan, T. Denoeux, An evidential classifier based on feature selection and two-step classification strategy, *Pattern Recognit.* 48 (2015) 2318–2327.
- [25] Z. Liu, Q. Pan, J. Dezert, A. Martin, Adaptive imputation of missing values for incomplete pattern classification, *Pattern Recognit.* 52 (2016) 85–95.
- [26] T. Denoeux, O. Kanjanatarakul, S. Sriboonchitta, EK-NNclus: a clustering procedure based on the evidential K-nearest neighbor rule, *Knowl.-Based Syst.* 88 (2015) 57–69.

- [27] Z. Liu, Q. Pan, J. Dezert, G. Mercier, Credal c-means clustering method based on belief functions, *Knowl.-Based Syst.* 74 (2015) 119–132.
- [28] Z. Liu, J. Dezert, G. Mercier, Q. Pan, Belief c-means: an extension of fuzzy C-means algorithm in belief functions framework, *Pattern Recognit. Lett.* 33 (3) (2012) 291–300.
- [29] F. Smarandache, *A Unifying Field in Logics: Neutrosophy. Neutrosophic Probability, Set, and Logic*, American Research Press, Rehoboth, 1999.
- [30] F. Smarandache, *Introduction to Neutrosophic Statistics*, Sitech & Education Publishing, Craiova, Romania & Columbus, U.S.A., 2014.
- [31] F. Smarandache, *Introduction to Neutrosophic Measure, Neutrosophic Integral, and Neutrosophic Probability*, Sitech & Education Publishing, Romania & U.S.A., 2014.
- [32] X. Li, D. Jean, X. Huang, Z. Meng, X. Wu, A fast approximate reasoning method in hierarchical DSMT(A), *Acta Electron. Sin.* 38 (11) (2010) 2566–2572.
- [33] P. Djiknavorian, D. Grenier, Reducing DSMT hybrid rule complexity through optimization of the calculation algorithm, in: *Advances and Application of DSMT for Information Fusion*, vol. 2, Amer. Res. Press, Rehoboth, 2006, pp. 365–429, Chap. 15.
- [34] A. Martin, Implementing general belief function framework with a practical codification for low complexity, in: *Advances and Application of DSMT for Information Fusion*, vol. 3, Amer. Res. Press, Rehoboth, 2009, pp. 217–273, Chap. 7.
- [35] N. Abbas, Y. Chibani, H. Nemmour, Handwritten digit recognition based on a DSMT-SVM parallel combination, in: *Proc. 13th International Conference on Frontiers in Handwriting Recognition, ICFHR, Bari, Italy, September 18–20, 2012*, pp. 241–246.
- [36] X. Li, X. Wu, J. Sun, Z. Meng, An approximate reasoning method in Dezert-Smarandache theory, *J. Electron. (China)* 26 (6) (2009) 738–745.
- [37] X. Li, J. Dezert, F. Smarandache, X. Huang, Evidence supporting measure of similarity for reducing the complexity in information fusion, *Inf. Sci.* 181 (2011) 1818–1835.
- [38] N. Abbas, Y. Chibani, Z. Belhadi, M. Hedir, A DSMT based combination scheme for multi-class classification, in: *Proc. 16th International Conference on Information Fusion, ICI, Istanbul, Turkey, July 9–12, 2013*, pp. 1950–1957.
- [39] D.C. Zhang, C.M. Hou, L.Y. Wang, W.Q. Ji, Converging to a period-two solution in the recursive sequence, *Far East J. Appl. Math.* 73 (1) (2012) 17–24.
- [40] D.C. Zhang, L.Y. Wang, X.B. Li, S.W. Cui, The separable difference equation $x_{n+1} = \frac{bx_n}{ax_{n-1}}$, *Far East J. Appl. Math.* 86 (3) (2014) 263–268.
- [41] J. Dezert, F. Smarandache, DSMT: a new paradigm shift for information fusion, in: *Cogis06 International Conference, Paris, France, 2006*, pp. 15–17.
- [42] F. Smarandache, J. Dezert, Information fusion based on new proportional conflict redistribution rules, in: *Proceedings of Fusion 2005 Conf., Philadelphia, July 26–29, 2005*, pp. 907–914.
- [43] Anne-Laure Jousselme, et al., A new distance between two bodies of evidence, *Inf. Fusion* 2 (2) (2001) 91–101.
- [44] Q. Guo, Y. He, X. Guan, et al., An evidence clustering DSMT approximate reasoning method based on convex functions analysis, *Digit. Signal Process.* 45 (2015) 13–23.

Qiang Guo was born in Yantai, Shandong Province of China in 1986. He is the Lecturer in Research Institute of Information Fusion of Naval Aeronautical and Astronautical University, Yantai, Shandong Province, China. He received his B.E. degree in information engineering, his M.S. degree and his Ph.D. degree in information and communication engineering

from Naval Aeronautical and Astronautical University, Yantai, Shandong Province, China, in 2008, 2010 and 2015, respectively. His research interests are information fusion, evidential reasoning, big data, and signal processing.

You He is currently the Academician of Chinese Academy of Engineering, Head, Professor, Doctor Tutor of the Research Institute of Information Fusion of Naval Aeronautical and Astronautical University, Yantai, Shandong Province, China, as well as Part-time Professor of Tsinghua University, Beijing, China. He also serves as IET fellow, a managing director of Chinese Aviation Society, a fellow member of Chinese Institute of Electronics and a member in a large range of professional and social organizations. Moreover, he was the founder of the National Conference on Information Fusion, and served as General Chairman in 2009. He received his B.S. degree in electronic engineering and the M.S. degree in computer science from Huazhong University of Science and Technology at Wuhan, P.R. China, in 1982 and 1988, respectively. From October 1991 to November 1992, he was with the institute of Communication at Technical University of Braunschweig, Germany, where he carried out automatic radar detection theory and CFAR algorithm studies. From November 1992 to December 1994, he was an Associate Professor in the Department of Electronic Engineering at Technical University of Yantai, China. Then, he received the Ph.D. degree in communication and information systems from Tsinghua University, in 1997. His research interests are information fusion, signal processing, and so on.

Tao Jian is Associate Professor in Research Institute of Information Fusion of Naval Aeronautical and Astronautical University, Yantai, Shandong Province, China. He received his B.E. degree in radar engineering, his M.S. degree and his Ph.D. degree in signal and information processing from Naval Aeronautical and Astronautical University, Yantai, Shandong Province, China, in 2003, 2006 and 2011, respectively. His research interests are radar signal and information processing.

Haipeng Wang is the Lecturer in Research Institute of Information Fusion of Naval Aeronautical and Astronautical University, Yantai, Shandong Province, China. He received his B.E. degree in radar engineering, his M.S. degree and his Ph.D. degree in information and communication engineering from Naval Aeronautical and Astronautical University, Yantai, Shandong Province, China, in 2006, 2008 and 2012, respectively. His research interests are information fusion, big data, and signal processing.

Shutao Xia is the Lecturer in Research Institute of Information Fusion of Naval Aeronautical and Astronautical University, Yantai, Shandong Province, China. He received his B.E. degree in electrical information engineering and his M.S. degree in information and communication engineering from Naval Aeronautical and Astronautical University, Yantai, Shandong Province, China, in 2003 and 2008, respectively. His research interests are information fusion, data processing and big data.